Medicinal
Plant Biology

REVIEW

Open Access

https://doi.org/10.48130/MPB-2023-0005
Medicinal Plant Biology **2023**, 2:5

Current progress of *Atractylodes macrocephala* Koidz.: A review of its biogeography, PAO-ZHI processing, biological activities, biosynthesis pathways, and technology applications

Ruiwen Yang[1#], Huiyan Fan[1#], Beihui He[1], Qingyan Ruan[1], Baoyu Wei[1], Bing Han[1], Xiaolong Hao[1], Itay Maoz[2] and Guoyin Kai[1*]

[1] *Jinhua Academy, Zhejiang Provincial International S&T Cooperation Base for Active Ingredients of Medicinal and Edible Plants and Health, Zhejiang Provincial Key TCM Laboratory for Chinese Resource Innovation and Transformation, Institute of Chinese Medicine Resource Innovation and Quality Evaluation, School of Pharmaceutical Sciences, Zhejiang Chinese Medical University, Hangzhou 310053, China*
[2] *Department of Postharvest Science, Agricultural Research Organization, Volcani Center, PO Box 15159, HaMaccabim Road 68, Rishon LeZion 7505101, Israel*
[#] These authors contributed equally: Ruiwen Yang, Huiyan Fan
[*] Corresponding author, E-mail: kaiguoyin@163.com

Abstract

The *Atractylodes macrocephala* Koidz. is a traditional Chinese rhizome herb, consumed for its well-known medicinal value. This review summarizes the recent research findings on biological activities, main biosynthesis pathways, PAO-ZHI processing, and technology application. The impact of biogeography led to significant differences in phenotypes and chemotypes. The PAO-ZHI processing also significantly affected *A. macrocephala* rhizome (AMR) bioactivity. A further systemic mechanistic investigation is required. Besides, new AMR polysaccharides with immunomodulatory effects, improving gastrointestinal function, and antitumor activity are constantly being isolated and characterized. Also, the discovery of novel families of compounds, such as the atractylenolides possessing antitumor, neuroprotective, immunomodulatory, and anti-inflammatory activities, is still ongoing work. Advanced genetics tools, such as in-depth transcriptomics, provide the basis for exploring *A. macrocephala* resources' functional genetic and molecular regulatory mechanisms. Still, some pathways are more elusive than others, and the biosynthetic pathways of sesquiterpenes, one of the prominent active families, still present a challenge in AMR and other plants. We propose here new directions and opportunities to advance current research in AMR. This review lays the theoretical foundation for fully developing and utilizing *A. macrocephala* resources.

Citation: Yang R, Fan H, He B, Ruan Q, Wei B, et al. 2023. Current progress of *Atractylodes macrocephala* Koidz.: A review of its biogeography, PAO-ZHI processing, biological activities, biosynthesis pathways, and technology applications. *Medicinal Plant Biology* 2:5 https://doi.org/10.48130/MPB-2023-0005

Introduction

Atractylodes macrocephala Koidz. (common names 'Baizhu' in Chinese and 'Byakujutsu' in Japanese) is a diploid (2n = 2x = 24) and out-crossing perennial herb in the *Compositae* family, and has a long history of cultivation in temperate and subtropical areas of East Asia as it is widely used in traditional herbal remedies with multiple pharmacological activities[1–3]. The 'Pharmacopoeia of the People's Republic of China' states that 'Baizhu' is the dry rhizome of *A. macrocephala* Koidz. (*Atractylodis Macrocephalae* Rhizoma, AMR). However, in Japanese traditional medicine 'Baizhu' can be referred to both: *A. japonica* or *A. macrocephala*[4].

A. macrocephala is naturally endemic to China and cultivated in more than 200 towns in China, belonging to Zhejiang, Hunan, Jiangxi, Anhui, Fujian, Sichuan, Hubei, Hebei, Henan, Jiangsu, Guizhou, Shanxi, and Shaanxi Provinces[3]. *A. macrocephala* grows to a height of 20–60 cm (Fig. 1). The leaves are green, papery, hairless, and generally foliole with 3–5 laminae with cylindric glabrous stems and branches. The flowers grow and aggregate into a capitulum at the apex of the stem. The corollas are purplish-red, and the florets are 1.7 cm long. The achenes, densely covered with white, straight hairs, are obconic and measure 7.5 mm long. The rhizomes used for medicinal purposes are irregular masses or irregularly curving cylinders about 3–13 cm long and 1.5–7 cm in diameter with an outwardly pale greyish yellow to pale yellowish color or a sparse greyish brown color. The periderm-covered rhizomes are externally greyish brown, often with nodose protuberances and coarse wrinkles. The cross-sections are white with fine dots of light yellowish-brown to brown secretion. Rhizomes are collected from plants that are > 2 years old during the spring. The fibrils are removed, dried, and used for medicinal purposes[5,6].

The medicinal properties of AMRs are used for spleen deficiency, phlegm drinking, dizziness, palpitation, edema, spontaneous sweating, benefit Qi, and fetal restlessness[7]. The AMR contains various functional components, among which high polysaccharide content, with a yield close to 30%[8]. Therefore, the polysaccharides of *A. macrocephala* Koidz. rhizome (AMRP) are essential in assessing the quality control and bioactivity of *A. macrocephala*. Volatile oil accounts for about 1.4% of AMR, with atractylon and atractylodin as the main components[9]. Atractylon can be converted to atractylenolide I (AT-I), atractylenolide II (AT-II), and atractylenolide III (AT-III) under

ambient conditions. AT-III can be dehydrated to AT-II under heating conditions[10,11]. AMRs, including esters, sesqui-, and triterpenes, have a wide range of biological activities, such as improving immune activity, intestinal digestion, neuroprotective activity, immune anti-inflammatory, and anti-tumor.

In recent years, research on the pharmacological aspects of AMR has continued to increase. Still, the discovery of the main active components in AMR is in its infancy. The PAO-ZHI processing of AMR is a critical step for AMR to exert its functional effects, but also, in this case, further work is required. Studies on the biosynthesis of bioactive compounds and different types of transcriptomes advanced current knowledge of *A. macrocephala*, but, as mentioned, required more systematic work. Ulteriorly, an outlook on the future research directions of *A. macrocephala* was provided based on the advanced technologies currently applied in *A. macrocephala* (Fig. 2).

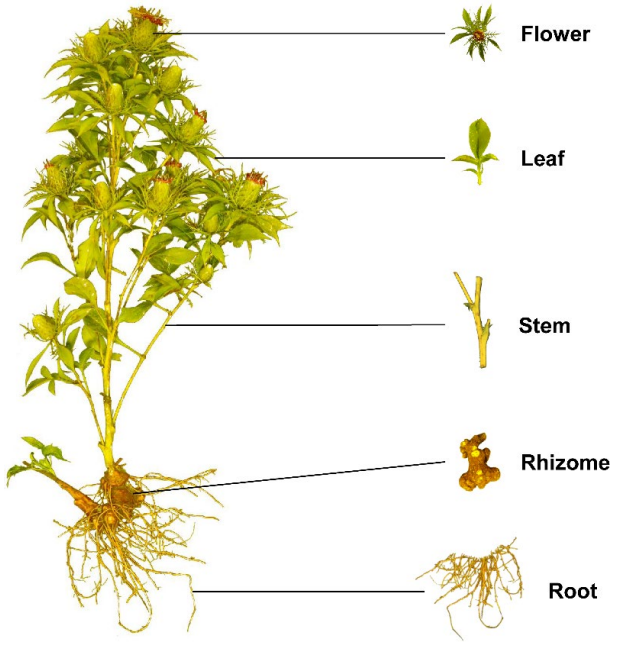

Fig. 1 Plant morphology of *A. macrocephala*.

Origin distribution and processing of *A. macrocephala*

Origin differentiation of *A. macrocephala*

A. macrocephala is distributed among mountainous regions more than 800 m above sea level along the middle and lower reaches of the Yangtze River (China)[5]. Due to over-exploitation and habitat destruction, natural populations are rare, threatened, and extinct in many locations[1,12]. In contrast to its native range, *A. macrocephala* is widely cultivated throughout China, in a total area of 2,000–2,500 ha, with a yield of 7,000 t of rhizomes annually[13]. *A. macrocephala* is mainly produced in Zhejiang, Anhui, and Hebei (China)[14]. Since ancient times, Zhejiang has been the famous producing area and was later introduced to Jiangxi, Hunan, Hebei, and other places[15]. Wild *A. macrocephala* is currently present in at least 14 provinces in China. It is mainly distributed over three mountain ranges, including the Tianmu and Dapan mountains in Zhejiang Province and the Mufu mountains along the border of Hunan and Jiangxi Provinces. *A. macrocephala* grows in a forest, or

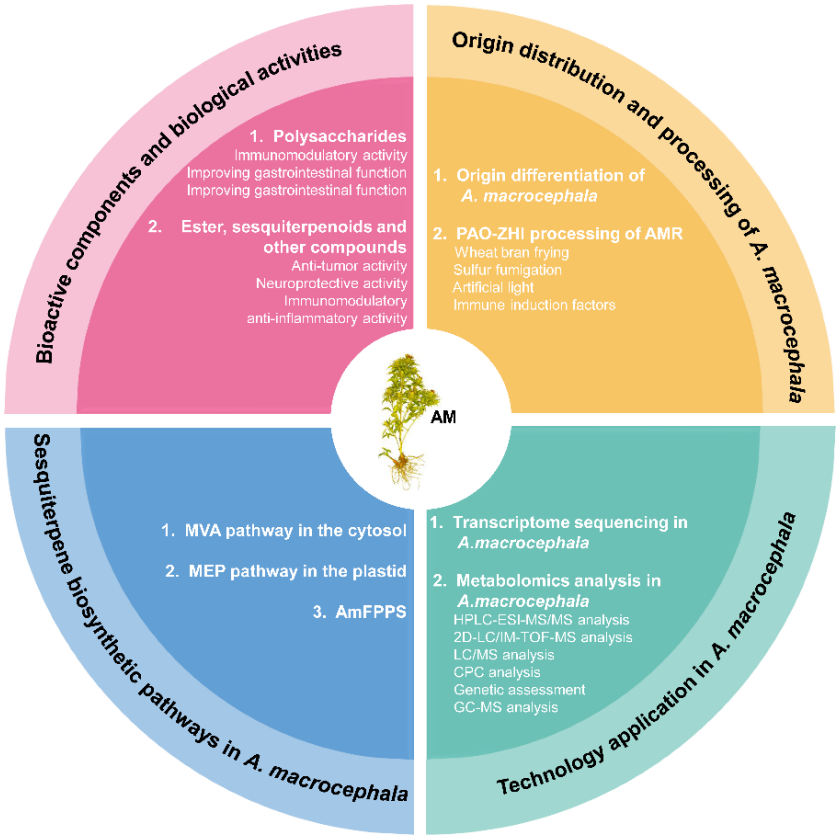

Fig. 2 Current progress of *A. macrocephala*.

grassy areas on mountain or hill slopes and valleys at an altitude of 600–2,800 m. *A. macrocephala* grows rapidly at a temperature of 22–28 °C, and favors conditions with total precipitation of 300–400 mm evenly distributed among the growing season[16]. Chen et al. first used alternating trilinear decomposition (ATLD) to characterize the three-dimensional fluorescence spectrum of *A. macrocephala*[17]. Then they combined the three-dimensional fluorescence spectrum with partial least squares discriminant analysis (PLS-DA) and k-nearest neighbor method (kNN) to trace the origin of Atractylodes samples. The results showed that the classification models established by PLS-DA and kNN could effectively distinguish the samples from three major Atractylodes producing areas (Anhui, Hunan, and Zhejiang), and the classification accuracy rate (CCR) of Zhejiang atractylodes was up to 80%, and 90%, respectively[17]. Zhang et al. compared the characteristics, volatile oil content, and chemical components of attested materials from six producing areas of Zhejiang, Anhui, Hubei, Hunan, Hebei, and Henan. Differences in the shape, size, and surface characteristics were reported, with the content of volatile oil ranging from 0.58% to 1.22%, from high to low, Hunan (1.22%) > Zhejiang (1.20%) > Anhui (1.02%) > Hubei (0.94%) > Henan (0.86%) > Hebei (0.58%)[18]. This study showed that the volatile oil content of *A. macrocephala* in Hunan, Anhui, and Hubei is not much different from that of Zhejiang, which is around 1%. *A. macrocephala* is a local herb in Zhejiang, with standardized cultivation techniques, with production used to reach 80%–90% of the country. However, in recent years, the rapid development of Zhejiang's real estate economy has reduced the area planted with Zhejiang *A. macrocephala*, resulting in a sudden decrease in production. Therefore, neighboring regions, such as Anhui and Hunan, vigorously cultivate *A. macrocephala*, and the yield and quality of *A. macrocephala* can be comparable to those of Zhejiang. The results were consistent with the data reports[18]. Guo et al. analyzed the differentially expressed genes of Atractylodes transcripts from different regions by the Illumina HiSeq sequencing platform. It was found that 2,333, 1,846, and 1,239 DEGs were screened from Hubei and Hebei, Anhui and Hubei, and Anhui and Hebei Atrexia, respectively, among which 1,424, 1,091, and 731 DEGs were annotated in the GO database. There were 432, 321, and 208 DEGs annotated in the KEGG database. These DEGs were mainly related to metabolic processes and metabolic pathways of secondary metabolites. The highest expression levels of these genes were found in Hubei, indicating higher terpenoid production in Hubei[19]. Other compounds were differentially accumulated in Atractylodes. Chlorogenic acid from Hebei was 0.22%, significantly higher than that from Zhejiang and Anhui[20]. Moreover, the content of neochlorogenic acid and chlorogenic acid decreased after processing, with the highest effect reported in Zhejiang, with the average transfer rate of neochlorogenic acid and chlorogenic acid reaching 55.68% and 55.05%[20]. All these changes would bring great help in distinguishing the origins of *A. macrocephala*.

PAO-ZHI processing of AMR

Medicinal AMR can be divided into raw AMR and cooked AMR. The processing method is PAO-ZHI; the most traditional method is wheat bran frying. The literature compared two different treatment methods, crude *A. macrocephala* (CA) and bran-processed *A. macrocephala*, and found that the pharmacological effects of AMR changed after frying with wheat bran, mainly in the anti-tumor, antiviral and anti-inflammatory effects[21]. The anti-inflammatory effect was enhanced, while the anti-tumor and antiviral effects were somewhat weakened, which may be related to the composition changes of the compounds after frying. The study of the content of AT-I, II, and III, and atractyloside A, in rat serum provided helpful information on the mechanism of wheat bran processing[22]. In addition to frying wheat bran, Sun et al. used sulfur fumigation to treat AMR[23]. They found that the concentration of different compounds changed, producing up to 15 kinds of terpenoids. Changes in pharmacological effects were related to treatment and the type of illumination[24,25]. Also, artificial light can improve the various biological functions. *A. macrocephala* grew better under microwave electrodeless light, with a chlorophyll content of 57.07 ± 0.65 soil and plant analyzer develotrnent (SPAD)[24]. The antioxidant activity of AMR extract treated with light-emitting diode (LED)-red light was the highest (95.3 ± 1.1%) compared with other treatments[24]. The total phenol and flavonoid contents of AMR extract treated with LED-green light were the highest at 24.93 ± 0.3 mg gallic acid equivalents (GAE)/g and 11.2 ± 0.3 mg quercetin equivalents (QE)/g compared with other treatments[24,25]. Polysaccharides from *Chrysanthemun indicum* L.[26] and *Sclerotium rolfsiisacc*[27] can improve AMR's biomass and bioactive substances by stimulating plant defense and thus affect their efficacy. In summary, there are compositional differences between *A. macrocephala* from different origins. Besides, different treatments, including processing mode, light irradiation, and immune induction factors, which can affect AMR's biological activity, provide some reference for the cultivation and processing of *A. macrocephala* (Fig. 3).

Bioactive components and biological activities

The AMR has been reported to be rich in polysaccharides, sesquiterpenoids (atractylenolides), volatile compounds, and polyacetylenes[3]. These compounds have contributed to various biological activities in AMR, including immunomodulatory effects, improving gastrointestinal function, anti-tumor activity, neuroprotective activity, and anti-inflammatory.

Polysaccharides

AMRP has received increasing attention as the main active component in AMR because of its rich and diverse biological activities. In the last five years, nine AMRP have been isolated from AMR. RAMP2 had been isolated from AMR, with a molecular weight of 4.354×10^3 Da. It was composed of mannose, galacturonic acid, glucose, galactose, and arabinose, with the main linkages of →3-β-glcp-(1→, →3,6-β-glcp-(1→, →6-β-glcp-(1→, T-β-glcp-(1→, →4-α-galpA-(1→, →4-α-galpA-6-OMe-(1→, →5-α-araf-(1→, →4,6-β-manp-(1→ and →4-β-galp-(1→[28]. Three water-soluble polysaccharides AMAP-1, AMAP-2, and AMAP-3 were isolated with a molecular weight of 13.8×10^4 Da, 16.2×10^4 Da, and 8.5×10^4 Da, respectively. Three polysaccharides were deduced to be natural pectin-type polysaccharides, where the homogalacturonan (HG) region consists of α-(1→4)-linked GalpA residues and the ramified region consists of alternating α-(1→4)-linked GalpA residues and α-(1→2)-linked Rhap residues. Besides, three polysaccharides were composed of different ratios of HG and rhamnogalacturonan type I (RG-I) regions[29]. Furthermore, RAMPtp has been extracted from AMR with a molecular weight of 1.867×10^3 Da. It consists of

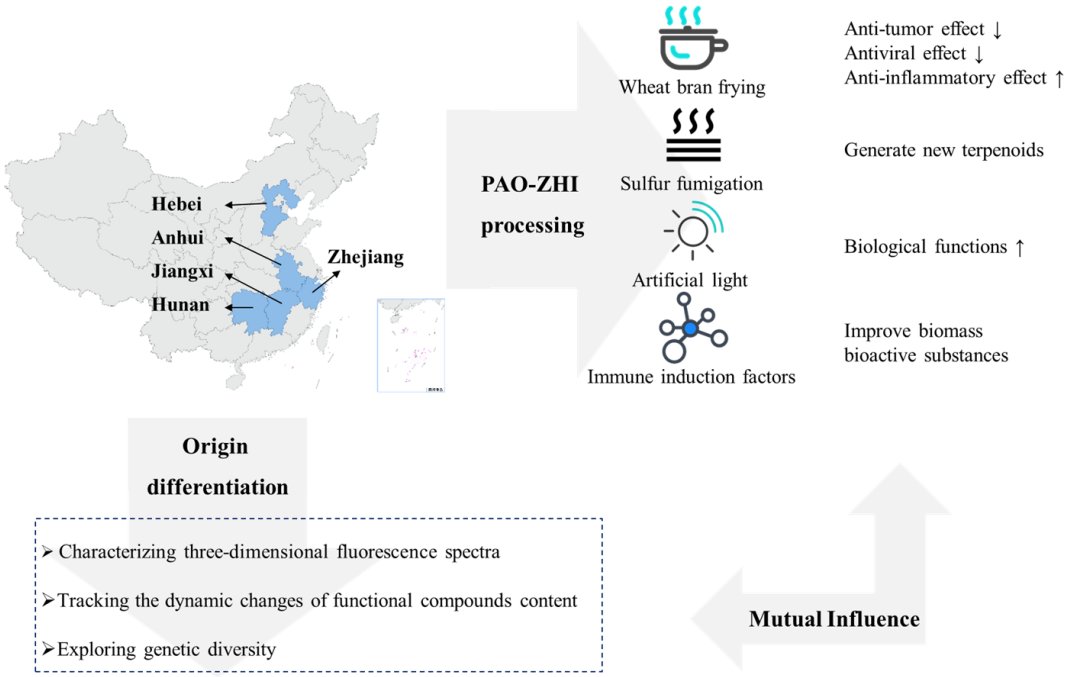

Fig. 3 Origin, distribution and processing of *A. macrocephala*.

glucose, mannose, rhamnose, arabinose, and galactose with 60.67%, 14.99%, 10.61%, 8.83%, and 4.90%, connected by 1,3-linked β-D Galp and 1,6-linked β-D Galp residues[30]. Additionally, PAMK was characterized by a molecular weight of 4.1 kDa, consisting of galactose, arabinose, and glucose in a molar ratio of 1:1.5:5, with an alpha structure and containing 96.47% polysaccharide and small amounts of protein, nucleic acid, and uric acid[31]. Another PAMK extracted from AMR had a molecular weight of 2.816×10^3 Da and consisted of glucose and mannose in molar ratios of 0.582 to 0.418[32]. Guo et al. isolated PAMK with a molecular weight of 4.748×10^3 g/mol from AMR, consisting of glucose, galactose, arabinose, fructose, and mannose in proportions of 67.01%, 12.32%, 9.89%, 1.18%, and 0.91%, respectively[33]. In addition, AMP1-1 is a neutral polysaccharide fragment with a molecular weight of 1.433 kDa isolated from AMR. It consists of glucose and fructose, and the structure was identified as inulin-type fructose α-D-Glcp-1→(2-β-D-Fruf-1)$_7$[34]. These reports indicated that, in general, polysaccharides are extracted by water decoction, ultrasonic-assisted extraction, enzyme hydrolysis method, and microwave-assisted extraction. The separation and purification are column chromatography, stepwise ethanol precipitation, and ultrafiltration. Their physicochemical properties and structural characterization are generally achieved by determining the molecular weight, determining the monosaccharide composition, analyzing the secondary structure, and glycosidic bond configuration of polysaccharides with Fourier transform infrared (FT-IR) and nuclear magnetic resonance (NMR). The advanced structures of polysaccharides can be identified by high-performance size exclusion chromatography-multiangle laser light scattering (HPSEC-MALLS), transmission electron microscopy (TEM), and scanning electron microscopy (SEM) techniques (Table 1). AMRP has various physiological functions, including immunomodulatory effects, improving gastrointestinal function, and anti-tumor activity. The related biological activities, animal models, monitoring indicators, and results are summarized in Table 1.

Immunomodulatory activity

To study the immunomodulatory activity of AMRP, the biological models generally adopted are chicken, goose, mouse, and human cell lines. Experiments based on the chicken model have generally applied 200 mg/kg doses. It was reported that AMRP protected the chicken spleen against heat stress (HS) by alleviating the chicken spleen immune dysfunction caused by HS, reducing oxidative stress, enhancing mitochondrial function, and inhibiting cell apoptosis[35]. Selenium and AMRP could improve the abnormal oxidation and apoptosis levels and endoplasmic reticulum damage caused by HS, and could act synergistically in the chicken spleen to regulate biomarker levels[36]. It indicated that AMRP and the combination of selenium and AMRP could be applied as chicken feed supplementation to alleviate the damage of HS and improve chicken immunity.

The general application dose in the goose model is also 200 mg/kg, and the main injury inducer is cyclophosphamide (CTX). AMRP alleviated CTX-induced immune damage in geese and provided stable humoral immune protection[37]. Little is known about the role of AMRP in enhancing immunity in geese through the miRNA pathway. It was reported that AMRP alleviated CTX-induced decrease in T lymphocyte activation levels through the novel _mir2/CTLA4/CD28/AP-1 signaling pathway[38]. It was also reported that AMRP might be achieved by upregulating the TCR-NFAT pathway through novel_mir2 targeting of CTLA4, thereby attenuating the immune damage induced by CTX[39]. This indicated that AMRP could also be used as goose feed supplementation to improve the goose's autoimmunity.

The typical injury inducer for mouse models is CTX, and the effects on mouse spleen tissue are mainly observed. BALB/c female mice were CTX-induced damage. However, AMRP

Table 1. Components and bioactivity of polysaccharides from *Atractylodes macrocephala* Koidz. Rhizome.

Pharmacological activities	Detailed function	Polysaccharides information	Model	Dose	Test index	Results	Ref.
Immunomodulatory effects	Restore immune function	/	Chicken models (HS-induced)	200 mg/kg	Oxidative index; Activities of mitochondrial complexes and ATPases; Ultrastructure in chicken spleens; Expression levels of cytokines, Mitochondrial dynamics- and apoptosis-related genes	**Alleviated** the expression of IL-1 ↑,TNF-α ↑, IL-2 ↓, IFN- γ ↓; mitochondrial dynamics- and anti-apoptosis-related genes ↓; pro-apoptosis-related genes ↑; the activities of mitochondrial complexes and ATPases ↓ **caused by HS**	[35]
	Regulate the immune function	/	Chicken models (HS-induced)	200 mg/kg	iNOS–NO activities; ER stress-related genes; Apoptosis-related genes; Apoptosis levels	**Alleviated** NO content ↑; activity of iNOS ↑ in the chicken spleen; GRP78, GRP94, ATF4, ATF6, IRE ↑; caspase3 ↑; Bcl-2 ↓ **caused by HS**	[36]
	Relieve immunosuppression	Commercial AMR powder (purity 70%)	Geese models (CTX-induced)	400 mg/kg	Spleen development; Percentages of leukocytes in peripheral blood	**Alleviated** the spleen damage; T and B cell proliferation ↓; imbalance of leukocytes; disturbances of humoral; cellular immunity **caused by CTX**	[37]
	Active the lymphocytes	Commercial AMR powder (purity 95%)	Geese models (CTX-induced)	400 mg/kg	Thymus morphology; The level of serum GMC-SF, IL-1b, IL-3, IL-5; mRNA expression of CD25, novel_mir2, CTLA4 and CD28 signal pathway	Maintain normal cell morphology of thymus; **Alleviated** GMC-SF ↓, IL-1b ↓, IL-5↓, IL-6↓, TGF-b↓; IL-4 ↑, IL-10 ↑; novel_mir2 ↓, CD25↓, CD28↓ in thymus and lymphocytes **caused by CTX**	[38]
	Alleviate immunosuppression	Commercial AMR powder (purity 70%)	Geese models (CTX-induced)	400 mg/kg	Thymus development; T cell proliferation rate; The level of CD28, CD96, MHC-II; IL-2 levels in serum; differentially expressed miRNAs	**Alleviated** thymus damage; T lymphocyte proliferation rate ↓; T cell activation ↓; IL-2 levels ↓ **caused by CTX**; **Promoted** novel_mir2 ↑; CTLA4 ↓; TCR-NFAT signaling pathway	[39]
	Alleviates T cell activation decline	Commercial AMR powder (purity 95%)	BALB/c female mice (CTX-induced)	200 mg/kg	Spleen index; Morphology, death, cytokine concentration of splenocytes; Th1/Th2 ratio, activating factors of lymphocytes; T cell activating factors; mRNA expression level in CD28 signal pathway	Improved the spleen index; Alleviated abnormal splenocytes morphology and death; Balance Th1/Th2 ratio; IL-2 ↑, IL-6 ↑, TNF-α ↑, IFN-γ ↑; mRNA levels of CD28, PLCγ-1, IP3R, NFAT, AP-1 ↑	[40]
	Immunoregulation and Immunopotentiation	Commercial AMR powder (purity 80%)	BMDCs (LPS-induced); Female BALB/c mice (ovalbumin as a model antigen)	/	Surface molecule expression of BMDCs; Cytokines secreted by dendritic cell supernatants; OVA-specific antibodies in serum; Cytokines in serum; Lymphocyte immunophenotype	Expression of CD80 and CD86 ↑; IL-1β ↑, IL-12 ↑, TNF-α↑ and IFN-γ ↑; OVA-specific antibodies in serum ↑; Secretion of cytokines ↑; Proliferation rate of spleen lymphocytes ↑; Activation of $CD3^+CD4^+$ and $CD3^+CD8^+$ lymphocytes	[46]
	Increase immune-response capacity of the spleen in mice	Commercial AMR powder (purity 70%)	BALB/c female mice	100, 200, 400 mg/kg	Spleen index; Concentrations of cytokines; mRNA and protein expression levels in TLR4 signaling	In the medium-PAMK group: IL-2, IL-4, IFN-c, TNF-a ↑; mRNA and protein expression of TLR4, MyD88, TRAF6, TRAF3, NF-κB in the spleen ↑	[41]
	Immunological activity	Commercial AMR powder (purity 80%)	Murine splenic lymphocytes (LPS or PHA-induced)	13, 26, 52, 104, 208 μg/mL	T lymphocyte surface markers	Lymphocyte proliferation ↑; Ratio of $CD4^+/CD8^+$ T cells ↑	[47]
	Immunomodulatory activity	Total carbohydrates content 95.66 %	Mouse splenocytes (Con A or LPS-induced)	25, 50, 100 μg/mL	Splenocyte proliferation; NK cytotoxicity; Productions of NO and cytokines; Transcription factor activity; Signal pathways and receptor	Promoted splenocyte proliferation; Cells enter S and G2/M phases; Ratios of T/B cells ↑; NK cytotoxicity ↑; Transcriptional activities of NFAT ↑; NF-κB, AP-1 ↑; NO, IgG, IL-1α, IL-1β, IL-2, IL-3, IL-4, IL-6, IL-10, IL-12p40, IL-12p70, IL-13, IFN-γ, TNF-α, G-CSF, GM-CSF, KC, MIP-1α, MIP-1β, RANTES, Eotaxin ↑	[42]

(to be continued)

Table 1. (continued)

Pharmacological activities	Detailed function	Polysaccharides information	Model	Dose	Test index	Results	Ref.
	Promote the proliferation of thymic epithelial cells	Contents of fucrhaara, galactose, glucose, fructose, and xylitol: 0.98%, 0.40%, 88.67%, 4.47%, and 5.47%	MTEC1 cells	50 μg/mL	Cell viability and proliferation; lncRNAs, miRNAs, and mRNAs expression profiles in MTEC1 cells	The differential genes were 225 lncRNAs, 29 miRNAs, and 800 mRNAs; Genes enriched in cell cycle, cell division, NF-κB signaling, apoptotic process, and MAPK signaling pathway	[44]
	Immunomodulatory activity	MW: 4.354×10^3 Da; Composed of mannose, galacturonic acid, glucose, galactose and arabinose; The main linkages are →3-β-glcp-(1→, →3,6-β-glcp-(1→, →6-β-glcp-(1→, T-β-glcp-(1→, →4-α-galpA-(1→, →4-α-galpA-6-OMe-(1→, →5-α-araf-(1→, →4,6-β-manp-(1→ and →4-β-galp-(1→	$CD4^+$ T cell	50, 100, 200 μg/mL	Molecular weight; Monosaccharide composition; Secondary structure; Surface topography; Effect on Treg cells	Treg cells percentage ↑; mRNA expressions of Foxp3, IL-10 and IL-2 ↑; STAT5 phosphorylation levels ↑; IL-2/STAT5 pathway	[28]
	Immunostimulatory activity	MW of AMAP-1, AMAP-2, and AMAP-3 were 13.8×10^4 Da, 16.2×10^4 Da and 8.5×10^4 Da; HG region consists of α-(1→4)-linked GalpA residues	RAW264.7 cells (LPS-induced)	80, 40, 200 μg/mL	Molecular weight; Total carbohydrate; Uronic acid contents; Secondary structure; Monosaccharide composition; Immunostimulatory activity	RG-I-rich AMAP-1 and AMAP-2 improved the release of NO	[29]
	Immunomodulatory effect	MW: 1.867×10^3 Da; Contents of glucose, mannose, rhamnose, arabinose and galactose: 60.67%, 14.99%, 10.61%, 8.83% and 4.90%	SMLN lymphocytes	25 μg/ml	Molecular weight; Monosaccharide composition; Ultrastructure; Intracellular Ca^{2+}concentration; Target genes; Cell cycle distribution	$[Ca^{2+}]_i$ ↑; More cells in S and G2/M phases; IFN-γ ↑, IL-17A ↑; mRNA expressions of IL-4 ↓	[30]
	Macrophage activation	Total carbohydrates content 95.66 %	RAW264.7 macrophages (LPS-induced)	25, 50, 100 μg/mL	Pinocytic activity; Phagocytic uptake; Phenotypic characterization; Cytokine production; Bioinformatics analysis; Transcription factor inhibition	IL-6, IL-10 and TNF-α ↑; CCL2 and CCL5 ↑; Pinocytic and phagocytic activity ↑; CD40, CD80, CD86, MHC-I, MHC-II ↑; NF-κB and Jak-STAT pathway	[43]
	Immunomodulatory effect	Total carbohydrates content 95.66 %	SMLN lymphocytes	25, 50, 100 μg/mL	Cytokine production; CD4+ and CD8+ lymphocytes; Target genes; Bioinformatics analysis; T and B lymphocyte proliferation; Receptor binding and blocking	IFN-γ, IL-1α, IL-21, IFN-α, CCL4, CXCL9, CXCL10 ↑; $CD4^+$ and $CD8^+$subpopulations proportions ↑; c-JUN, NFAT4, STAT1, STAT3 ↑; 67 differentially expressed miRNAs (55 ↑ and 12 ↓), associated with immune system pathways; Affect T and B lymphocytes	[45]
Improving gastrointestinal function	Relieve enteritis and improve intestinal flora disorder	Commercial AMR powder (purity 70%); Contents of fucrhaara, galactose, glucose, xylitol, and fructose: 0.98%, 0.40%, 88.67%, 4.47%, and 5.47%	Goslings (LPS-induced)	400 mg/kg	Serum CRP, IL-1β, IL-6, and TNF-α levels; Positive rate of IgA; TLR4, occludin, ZO-1, cytokines, and immunoglobulin mRNA expression; Intestinal flora of gosling excrement	**Relieved** IL-1β, IL-6, TNF-α levels in serum ↑; the number of IgA-secreting cells ↑; TLR4 ↑; tight junction occludin and ZO-1 ↓; IL-1β mRNA expression in the small intestine ↑; Romboutsia ↓ **caused by LPS**	[48]
	Ameliorate ulcerative colitis	MW: 2.391×10^4 Da; Composed of mannose, glucuronic acid, glucose and arabinose in a molar ratio of 12.05:6.02:72.29:9.64	Male C57BL/6J mice (DDS-induced)	10, 20, 40 mg/kg bw	Histopathological evaluation; Inflammatory mediator; Composition of gut microbiota; Feces and plasma for global metabolites profiling	*Butyricicoccus*, *Lactobacillus* ↑; *Actinobacteria*, *Akkermansia*, *Anaeroplasma*, *Bifidobacterium*, *Erysipelatoclostridium*, *Faecalibaculum*, *Parasutterella*, *Parvibacter*, *Tenericutes*, *Verrucomicrobia* ↓; **Changed** 23 metabolites in fecal content; 21 metabolites in plasma content	[49]

(to be continued)

Table 1. (continued)

Pharmacological activities	Detailed function	Polysaccharides information	Model	Dose	Test index	Results	Ref.
	Attenuate ulcerative colitis	/	Male SD rats (TNBS-induced); Co-culture BMSCs and IEC-6 cells	540 mg/kg (for rats); 400 μg/mL (for cell)	Histopathological analysis; Cell migration; Levels of cytokines	Potentiated BMSCs' effect on preventing colitis and homing the injured tissue, regulated cytokines; BMSCs and AMP promoted the migration of IEC	[52]
	Against intestinal mucosal injury	MW: 3.714×10^3 Da; Composed of glucose, arabinose, galactose, galacturonic acid, rhamnose and mannose with molar ratios of 59.09:23.22:9.32:4.70:2.07:1.59	Male C57BL/6 mice (DDS-induced)	100 mg/kg	Intestinal morphology; IL-6, TNF-α and IL-1β in serum; mRNA expression; Intestinal microbiota	**Alleviated** body weight ↓; colon length ↓; colonic damage **caused by DSS**; Over-expression of TNF-α, IL-1β, IL-6 ↓; Infiltration of neutrophils in colon ↓; Mucin 2 ↑; Tight junction protein Claudin-1 ↑; Harmful bacteria content ↓; Beneficial bacteria content ↑	[50]
	Against intestinal injury	Total carbohydrates 95.66 %	IECs (DDS-induced)	5, 25, 50 μg/mL	Cell proliferation and apoptosis; Expression levels of intercellular TJ proteins; lncRNA screening	Proliferation and survival of IECs ↑; Novel lncRNA ITSN1-OT1 ↑; Blocked the nuclear import of phosphorylated STAT2	[51]
Anti-tumor activity	Induce apoptosis in transplanted H22 cells in mice	MW: 4.1×10^3 Da; Neutral heteropolysaccharide composed of galactose, arabinose, and glucose with α-configuration (molar ratio, 1:1.5:5)	Female Kunming mice	100 and 200 mg/kg (for rats)	Secondary structure; Molecular weight; Molecular weight; Thymus index and Spleen index; Lymphocyte Subpopulation in peripheral blood; Cell cycle distribution	In tumor-bearing mice CD^{3+}, CD^{4+}, CD^{8+} ↓; B cells ↑	[31]
	Regulate the innate immunity of colorectal cancer cells	Commercial AMR powder (purity 70%)	C57BL/6J mice (MC38 cells xenograft model)	500 mg/kg	Expression of pro-inflammatory cytokines and secretion	IL-6, IFN-λ, TNF-α, NO ↑ through MyD88/TLR4-dependent signaling pathway; Survival duration of mice with tumors ↑; Prevent tumorigenesis in mice	[54]
	Induce apoptosis of Eca-109 cells	MW: 2.1×10^3 Da; Neutral hetero polysaccharide composed of arabinose and glucose (molar ratio, 1:4.57) with pyranose rings and α-type and β-type glycosidic linkages	Eca-109 cells	0.25, 0.5, 1, 1.5, 2.00 mg/mL	Cell morphology; Cell cycle arrest; Induction of apoptosis	Accelerate the apoptosis of Eca109 cells	[53]

'/' denotes no useful information found in the study.

increased cytokine levels and attenuated the CTX-induced decrease in lymphocyte activation levels through the CD28/IP3R/PLCγ-1/AP-1/NFAT signaling pathway[40]. It has also been shown that AMRP may enhance the immune response in the mouse spleen through the TLR4-MyD88-NF-κB signaling pathway[41].

Various cellular models have been used to study the immune activity of AMRP, and most of these studies have explored the immune activity with mouse splenocytes and lymphocytes. Besides, the commonly used damage-inducing agents are LPS, phytohemagglutinin (PHA), and concanavalin A (Con A).

In one study, the immunoreactivity of AMRP was studied in cultured mouse splenocytes. LPS and Con A served as controls. Specific inhibitors against mitogen-activated protein kinases (MAPKs) and NF-κB significantly inhibited AMRP-induced IL-6 production. The results suggested that AMRP-induced splenocyte activation may be achieved through TLR4-independent MAPKs and NF-κB signaling pathways[42]. Besides, AMRP isolated from AMR acting on LPS-induced RAW264.7 macrophages revealed that NF-κB and Jak-STAT signaling pathways play a crucial role in regulating immune response and immune function[43]. RAMP2 increased the phosphorylation level of STAT5 in Treg cells, indicating that RAMP2 could increase the number of Treg cells through the IL-2/STAT5 signaling pathway[28]. Furthermore, the relationship between structure and immune activity was investigated. Polysaccharides rich in RG-I structure and high molecular weight improved NO release from RAW264.7 cells. Conversly, polysaccharides rich in HG structure and low molecular weight did not have this ability, indicating that the immunoreactivity of the polysaccharide may be related to the side chain of RG-I region[29]. Moreover, the effect of AMRP on the expression profile of lncRNAs, miRNAs, and mRNAs in MTEC1 cells has also been investigated. The differentially expressed genes include lncRNAs, Neat1, and Limd1. The involved signaling pathways include cell cycle, mitosis, apoptotic process, and MAPK[44].

Xu et al. found that AMRP affects supramammary lymph node (SMLN) lymphocytes prepared from healthy Holstein cows. Sixty-seven differentially expressed miRNAs were identified based on microRNA sequencing and were associated with immune system pathways such as PI3K-Akt, MAPKs, Jak-STAT, and calcium signaling pathways. AMRP exerted immunostimulatory effects on T and B lymphocytes by binding to T cell receptor (TCR) and membrane Ig alone, thereby mobilizing immune regulatory mechanisms within the bovine mammary gland[45].

AMRP can also be made into nanostructured lipid carriers (NLC). Nanoparticles as drug carriers can improve the action of drugs *in vivo*. NLC, as a nanoparticle, has the advantages of low toxicity and good targeting[46]. The optimization of the AMRP-NLC preparation process has been reported. The optimum technologic parameters were: the mass ratio of stearic acid to caprylic/capric triglyceride was 2:1. The mass ratio of poloxamer 188 to soy lecithin was 2:1. The sonication time was 12 min. The final encapsulation rate could reach 76.85%[47]. Furthermore, AMRP-NLC interfered with the maturation and differentiation of bone marrow-derived dendritic cells (BMDCs). Besides, AMRP-NLC, as an adjuvant of ovalbumin (OVA), could affect ova-immunized mice with enhanced immune effects[46].

Improving gastrointestinal function

AMRP also has the effect of alleviating intestinal damage. They are summarized in Table 1. The common damage-inducing agents are lipopolysaccharide (LPS), dextran sulfate sodium (DDS), and trinitrobenzene sulfonic acid (TNBS). A model of LPS-induced enteritis in goslings was constructed to observe the effect of AMRP on alleviating small intestinal damage. Gosling excrement was analyzed by 16S rDNA sequencing to illuminate the impact of AMRP on the intestinal flora. Results indicated that AMRP could maintain the relative stability of cytokine levels and immunoglobulin content and improve intestinal flora disorder[48]. Feng et al. used DDS-induced ulcerative colitis (UC) in mice and explored the alleviating effects of AMRP on UC with 16S rDNA sequencing technology and plasma metabolomics. The results showed that AMRP restored the DDS-induced disruption of intestinal flora composition, regulated the production of metabolites such as short-chain fatty acids and cadaveric amines, and regulated the metabolism of amino acids and bile acids by the host and intestinal flora[49]. A similar study has reported that AMRP has a protective effect on the damage of the intestinal mucosal barrier in mice caused by DSS. It was found that AMRP increased the expression of Mucin 2 and the tight junction protein Claudin-1. In addition, AMRP decreased the proportion of harmful bacteria and increased the potentially beneficial bacteria content in the intestine[50]. The protective effect of AMRP on DSS-induced damage to intestinal epithelial cells (IECs) has also been investigated. The results showed that AMRP promoted the proliferation and survival of IECs.

In addition, AMRP induced a novel lncRNA ITSN1-OT1, which blocked the nuclear import of phosphorylated STAT2 and inhibited the DSS-induced reduced expression and structural disruption of tight junction proteins[51]. AMRP can also act in combination with cells to protect the intestinal tract. The ulcerative colitis model in Male Sprague-Dawley (SD) rats was established using TNBS, and BMSCs were isolated. IEC-6 and BMSCs were co-cultured and treated by AMRP. The results showed that AMRP enhanced the prevention of TNBS-induced colitis in BMSCs, promoted the migration of IEC, and affected the expression of various cytokines[52]. These reports indicated that the 16S rDNA sequencing technique could become a standard method to examine the improvement of gastrointestinal function by AMRP.

Anti-tumor activity

AMRP has anti-tumor activity and other biological activities. AMRP can induce apoptosis in Hepatoma-22 (H22) and Eca-109 cells and modulate the innate immunity of MC38 cells. For instance, the anti-tumor effects of AMRP were investigated by constructing a tumor-bearing mouse model of H22 tumor cells. AMRP blocked the S-phase of H22 tumor cells and induced an immune response, inhibiting cell proliferation[31]. In addition, AMRP can inhibit cell proliferation through the mitochondrial pathway and by blocking the S-phase of Eca-109 tumor cells[53]. AMRP affects MC38 tumor cells, and the anti-tumor effect of AMRP was investigated with Toll-like receptor 4 (TLR4) KO C57BL/6 mice and the construction of the MC38 tumor cell xenograft model. AMRP significantly inhibited the development of MC38 cells in mice and prolonged the survival of tumor-bearing mice. AMRP activity was diminished in TLR4 KO mice. Combined with the immunoblotting assay results, it was shown that TLR4 regulated the MyD88-dependent signaling pathway, which has a critical effect on the anti-tumor effect of AMRP[54].

Esters, sesquiterpenoids, and other compounds

AMR contains a large number of bioactive compounds. Among them, small molecule compounds include esters, sesquiterpenes, and other compounds. These small molecule compounds have significant pharmacological activities, including anti-tumor, neuroprotective, immunomodulatory, and anti-inflammatory. In the last five years, small molecule compounds have been increasingly identified (Fig. 4), with atractylenolides as the main component of AMR extracts[11]. Atractylenolides are a small group of sesquiterpenoids. Atractylenolides include AT-I, AT-II, and AT-III, lactones isolated from AMR.

Anti-tumor activity

The anti-tumor activity was mainly manifested by AT-I and AT-II, especially AT-I (Table 2). Anti-tumor activity has been studied primarily *in vivo* and *in vitro*. However, there is a lack of research on the anti-tumor activity of atractylenolide in human clinical trials. The concentration of atractylenolide applied on cell lines was < 400 μM, or < 200 mg/kg on tumor-bearing mice.

AT-III affects human colorectal cancer. AT-II affects human gastric carcinoma and mammary tumorigenesis. AT-I affects human colon adenocarcinoma, human ovarian cancer, metastatic properties transfer of Cancer stem cells (CSCs), colorectal cancer, and human lung cancer, and enhances the sensitivity of triple-negative breast cancer cells to paclitaxel. Current techniques have made it possible to study the effects of atractylenolide on tumors at the signaling pathway level (Table 2). For instance, AT-III significantly inhibited the growth of HCT-116 cells and induced apoptosis by regulating the Bax/Bcl-2 apoptotic signaling pathway. In the HCT116 xenograft mice model, AT-III could inhibit tumor growth and regulate the expression of related proteins or genes. It indicated that AT-III could potentially treat human colorectal cancer[55]. AT-II significantly inhibited the proliferation and motility of HGC-27 and AGS cells and induced apoptosis by regulating the Akt/ERK signaling

Table 2. Anti-tumor activity of atractylenolides.

Types	Substances	Model	Index	Dose	Signal pathway	Results	Ref.
Human colorectal cancer	AT-III	HCT-116 cell; HCT-116 tumor xenografts bearing in nude mice	Cell viability; Cell apoptotic; mRNAs and protein expressions of Bax, Bcl-2, caspase-9 and caspase-3	25, 50, 100, 200 μM (for cell); 50, 100, 200 mg/kg (for rats)	Bax/Bcl-2 signaling pathway	Promoting the expression of proapoptotic related gene/proteins; Inhibiting the expression of antiapoptotic related gene/protein; Bax↑; Caspase-3↓; p53↓; Bcl-2↓	[55]
Human gastric carcinoma	AT-II	HGC-27 and AGS cell	Cell viability; Morphological changes; Flow cytometry; Wound healing; Cell proliferation, apoptosis, and motility	50, 100, 200, 400 μM	Akt/ERK signaling pathway	Cell proliferation, motility↓; Cell apoptosis↑; Bax↑; Bcl-2↓; p-Akt↓; p-ERK↓	[56]
Mammary tumorigenesis	AT-II	MCF 10A cell; Female SD rats (NMU-induced)	Nrf2 expression and nuclear accumulation; Cytoprotective effects; Tumor progression; mRNA and protein levels of Nrf2; Downstream detoxifying enzymes	20, 50, 100 μM (for cell); 100 and 200 mg/kg (for rats)	JNK/ERK-Nrf2-ARE signaling pathway; Nrf2-ARE signaling pathway	Nrf2 expressing↑; Nuclear translocation↑; Downstream detoxifying enzymes↓; 17*β*-Estradiol↓; Induced malignant transformation	[57]
Human colon adenocarcinoma	AT-I	HT-29 cell	Cell viability; TUNEL and Annexin V-FITC/PI double stain; Detection of initiator and executioner caspases level	10, 20, 40, 80, 100 μM	Mitochondria-dependent pathway	Pro-survival Bcl-2↓; Bax↑; Bak↑; Bad↑; Bim↑; Bid↑; Puma↑	[58]
Sensitize triple-negative TNBC cells to paclitaxel	AT-I	MDA-MB-231 cell; HS578T cell; Balb/c mice (MDA-MB-231 cells-implanted)	Cell viability Transwell migration CTGF expression	25, 50, 100 μM (for cell); 50 mg/kg (for rats)	/	Expression and secretion of CTGF↓; CAF markers↓; Blocking CTGF expression and fibroblast activation	[59]
Human ovarian cancer	AT-I	A2780 cell	Cell cycle; Cell apoptosis; Cyclin B1 and CDK1 level	12.5, 25, 50, 100 and 200 μM	PI3K/Akt/mTOR signaling pathway	Cyclin B1, CDK1↓; Bax↑; Caspase-9↓; Cleaved caspase-3↓; Cytochrome c↑; AIF↑; Bcl-2↓; Phosphorylation level of PI3K, Akt, mTOR↓	[60]
Impaired metastatic properties transfer of CSCs	AT-I	LoVo-CSCs; HT29-CSCs	Cell migration and invasion; miR-200c expression; Cell apoptosis	200 μM	PI3K/Akt/mTOR signaling pathway	Suppressing miR-200c activity; Disrupting EV uptake by non-CSCs	[61]
Colorectal cancer	AT-I	HCT116 cell; SW480 cell; male BALB/c nude mice (HCT116-implanted)	Cell viability; Cell apoptosis; Glucose uptake; Lactate Production; STAT3 expression; Immunohistological analysis	25, 50, 100, 150, 200 μM (for cell); 50 mg/kg (for rats)	JAK2/STAT3 signaling	Caspase-3↑; PARP-1↓; Bax↑; Bcl-2↓; Rate-limiting glycolytic enzyme HK2↓; STAT3 phosphorylation↓	[62]
Human lung cancer	AT-I	NSCLC cells (A549 and H1299); female nude mice (A549-Luc cells-implanted)	Cell viability; Cell cycle; Phosphorylation and protein expression of ERK1/2, Stat3, PDK1, transcription factor SP1; mRNA levels of *PDK1* gene	12.5, 25, 50, 100, 150 μM (for cell); 25 and 75 mg/kg (for rats)	/	ERK1/2↑; Stat3↓; SP1↓; PDK1↓	[63]

'/' denotes no useful information found in the study.

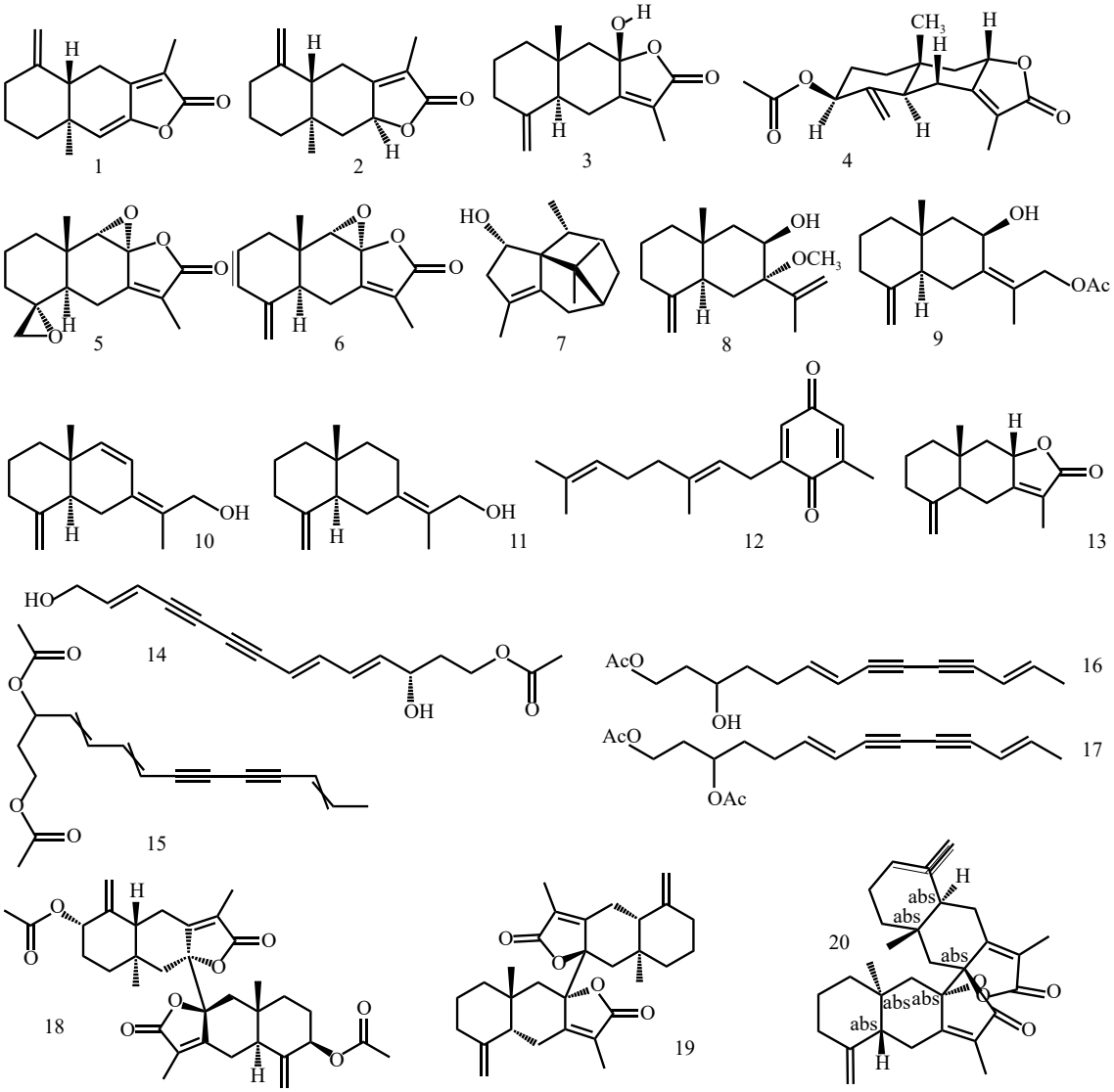

Fig. 4 Structure of small molecule compounds with bioactivities from AMR. Atractylenolide I (1); Atractylenolide II (2); Atractylenolide III (3); 3β-acetoxyl atractylenolide I (4); 4R,5R,8S,9S-diepoxylatractylenolide II (5); 8S,9S-epoxyla-tractylenolide II (6); Atractylmacrols A (7); Atractylmacrols B (8); Atractylmacrols C (9); Atractylmacrols D (10); Atractylmacrols E (11); 2-[(2E)-3,7-dimethyl-2,6-octadienyl]-6-methyl-2,5-cyclohexadiene-1,4-dione (12); 8-epiasterolid (13); (3S,4E,6E,12E)-1-acetoxy-tetradeca-4,6,12-triene-8,10-diyne-3,14-diol (14); (4E,6E,12E)-tetradeca-4,6,12-triene-8,10-diyne-13,14-triol (15); 1-acetoxy-tetradeca-6E,12E-diene-8, 10-diyne-3-ol (16); 1,3-diacetoxy-tetradeca-6E, 12E-diene-8,10-diyne (17); Biatractylenolide II (18); Biepiasterolid (19); Biatractylolide (20).

pathway. It suggested that AT-II can potentially treat gastric cancer[56]. However, in this study, the anti-tumor effects of AT-II *in vivo* were not examined. AT-II regulated intracellular-related enzyme expression in MCF 10A cells through the JNK/ERK-Nrf2-ARE signaling pathway. AT-II reduced inflammation and oxidative stress in rat mammary tissue through the Nrf2-ARE signaling pathway. AT-II inhibited tumor growth in the N-Nitroso-N-methyl urea (NMU)-induced mammary tumor mice model, indicating that AT-II can potentially prevent breast cancer[57]. AT-I induced apoptosis in HT-29 cells by activating anti-survival Bcl-2 family proteins and participating in a mitochondria-dependent pathway[58]. It indicated that AT-I is a potential drug effective against HT-29 cells. However, the study was only conducted *in vitro*; additional *in vivo* experimental data are needed. AT-I can enhance the sensitivity of triple-negative breast cancer (TNBC) cells to paclitaxel. MDA-MB-231 and HS578T cell co-culture systems were constructed, respectively. AT-I was found to impede TNBC cell migration. It also enhanced the sensitivity of TNBC cells to paclitaxel by inhibiting the conversion of fibroblasts into cancer-associated fibroblasts (CAFs) by breast cancer cells. In the MDA-MB-231 xenograft mice model, AT-I was found to enhance the effect of paclitaxel on tumors and inhibit the metastasis of tumors to the lung and liver[59]. AT-I inhibited the growth of A2780 cells through PI3K/Akt/mTOR signaling pathway, promoting apoptosis and blocking the cell cycle at G2/M phase change, suggesting a potential therapeutic agent for ovarian cancer[60]. However, related studies require *in vivo* validation trials. CSCs are an important factor in tumorigenesis. CSCs isolated from colorectal cancer (CRC) cells can metastasize to non-CSCs *via* miR-200c encapsulated in extracellular vesicles (EVs).

In contrast, AT-I could inhibit the activity and transfer of miR-200c. Meanwhile, interfere with the uptake of EVs by non-CSCs. This finding contributes to developing new microRNA-based

natural compounds against cancer[61]. AT-I has the function of treating colorectal cancer. HCT116 and SW480 cells were selected for *in vitro* experiments, and AT-I was found to regulate STAT3 phosphorylation negatively. The HCT116 xenograft mice model was constructed, and AT-I was found to inhibit the growth of HCT116. AT-I induced apoptosis in CRC cells, inhibited glycolysis, and blocked the JAK2/STAT3 signaling pathway, thus exerting anti-tumor activity[62]. The *in vitro* experiments were performed with A549 and H1299 cell lines. The *in vivo* experiments were performed to construct the A549-Luc xenograft mice model. The results showed that AT-I inhibited lung cancer cell growth by activating ERK1/2. AT-I inhibited SP1 protein expression and phosphorylation of Stat3, decreasing PDK1 gene expression. The study showed that AT-I could inhibit lung cancer cell growth and targeting PDK1 is a new direction for lung cancer treatment[63]. The research on the anti-tumor of atractylenolide is relatively complete, and there are various signaling pathways related to its anti-tumor activity. Based on the above information, the anti-tumor mechanism of atractylenolide in the past five years was schemed (Fig. 5).

Neuroprotective activity

In recent years, few studies have been conducted on the neuroprotective activity of esters or sesquiterpenoids from AMR. The neuroprotective effects of AT-III have been studied systematically. Biatractylolide has also been considered to have a better neuroprotective effect. New compounds continue to be identified, and their potential neuroprotective effects should be further explored. The related biological activities, animal models, monitoring indicators, and results are summarized in Table 3. Neuroprotective effects include the prevention and treatment of various diseases, such as Parkinson's, Alzheimer's, anti-depressant anxiety, cerebral ischemic injury, neuroinflammation, and hippocampal neuronal damage. *In vivo* and *in vitro* will shed light on the potential effect of sesquiterpenoids from AMR and other medicinal plants.

Zhang et al. identified eight compounds from AMR, two newly identified, including 3β-acetoxyl atractylenolide I and (3S,4E,6E,12E)-1-acetoxy-tetradecane-4,6,12-triene-8,10-diyne-3,14-diol. 1-Methyl-4-phenylpyridinium (MPP^+) could be used to construct a model of Parkinson's disease. A model of MPP^+-induced damage in SH-SY5Y cells was constructed. All eight compounds showed inhibitory effects on MPP^+-induced damage[64]. Si et al. newly identified eight additional sesquiterpenoids from AMR. A model of LPS-induced BV-2 cell injury was constructed. 4R, 5R, 8S, 9S-diepoxylatractylenolide II and 8S, 9S-epoxylatractylenolide II had significant anti-neuroinflammatory effects. Besides, the anti-inflammatory effect of 4R, 5R, 8S, 9S-diepoxylatractylenolide II might be related to the NF-κB signaling pathway[65]. Biatractylolide has a preventive effect against Alzheimer's disease. *In vitro* experiments were conducted by constructing an A$\beta_{25\text{-}35}$-induced PC12 cell injury model. *In vivo* experiments were conducted by constructing an A$\beta_{25\text{-}35}$-induced mice injury model to examine rats' spatial learning and memory abilities. Biatractylolide reduced hippocampal apoptosis, alleviated A$\beta_{25\text{-}35}$-induced neurological injury, and reduced the activation of the NF-κB signaling pathway. Thus, it can potentially treat Aβ-related lesions in the central nervous system[66]. It has also been shown that biatractylolide has neuroprotective effects *via* the PI3K-Akt-GSK3β-dependent pathway to alleviate glutamate-induced damage in PC12 and SH-SY5Y cells[67]. The attenuating inflammatory effects of AT-I were examined by constructing *in vivo* and *in vitro* Parkinson's disease models. Furthermore, AT-I alleviated LPS-induced BV-2 cell injury by reducing the nuclear translocation of NF-κB. AT-I restored 1-methyl-4-phenyl-1,2,3,6-tetrahydropyridine (MPTP)-induced behavioral impairment in C57BL6/J mice, protecting dopaminergic neurons[68]. AT-I also has anti-depressant effects. Chronic unpredictable mild stress (CUMS) induced depressive behavior in institute of cancer research (ICR) mice, and AT-I achieved anti-depressant function by inhibiting the activation of NLRP3 inflammatory vesicles, thereby reducing IL-1β content levels[69]. Biatractylenolide II is a newly identified sesquiterpene compound with the potential for treating Alzheimer's disease. The AChE inhibitory activity of

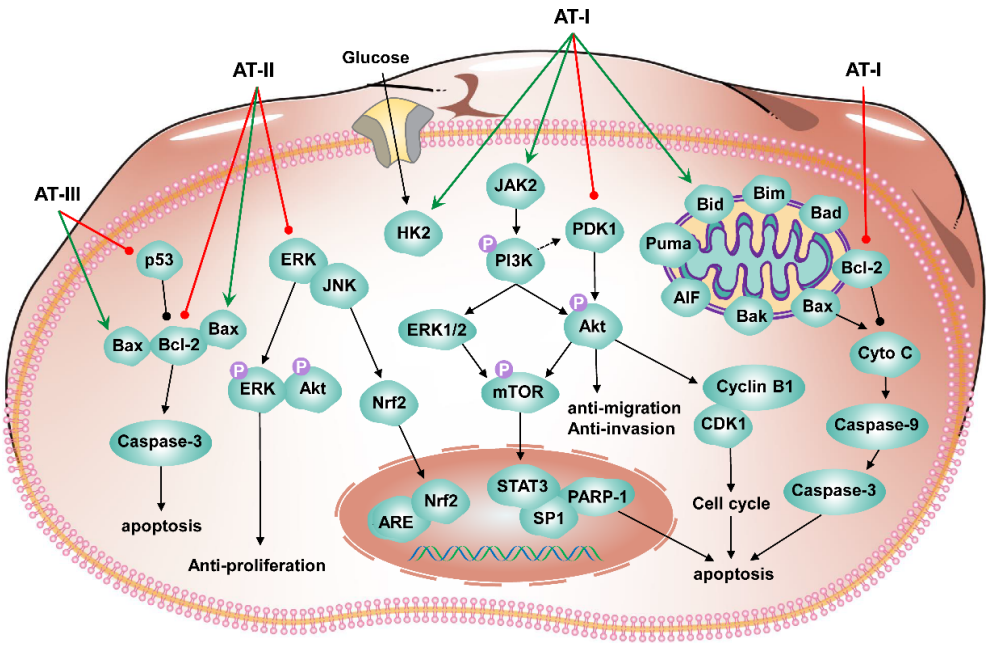

Fig. 5 Schematic diagram for the anti-tumor mechanism of atractylenolides.

Table 3. Neuroprotective effects of esters and sesquiterpenoids.

Activities	Substances	Model	Index	Dose	Signal pathway	Results	Ref.
Establish a PD model	AT-II; AT-I; Biepiasterolid; Isoatractylenolide I; AT-III; 3β-acetoxyl atractylenolide I; (4E,6E,12E)- tetradeca-4,6,12-triene-8,10-diyne-13,14-triol; (3S,4E,6E,12E)-1-acetoxy-tetradeca-4,6,12-triene-8,10-diyne-3,14-diol	SH-SY5Y cell (MPP^+-induced)	Cell viability	10, 1, 0.1 μM	/	All compounds have inhibitory activity on MPP^+-induced SH-SY5Y cell	[64]
/	4R,5R,8S,9S-diepoxylatractylenolide II; 8S,9S-epoxyla-tractylenolide II	BV-2 microglia cells (LPS-induced)	Cell viability; NO synthase inhibitor; IL-6 levels	6.25, 12.5, 25, 50, 100 μM	NF-κB signaling pathway	NO inhibition with IC50 values of 15.8, and 17.8 μM, respectively; IL-6 ↓	[65]
Protecting Alzheimer's disease	Biatractylolide	PC12 cell ($A\beta_{25\text{-}35}$-induced); Healthy male Wistar rats ($A\beta_{25\text{-}35}$-induced)	Cell viability; Morris water maze model; TNF-α, IL-6, and IL-1β	20, 40, 80 μM (for cells); 0.1, 0.3, 0.9 mg/kg (for rats)	NF-κB signaling pathway	Reduce apoptosis; Prevent cognitive decline; Reduce the activation of NF-κB signal pathway	[66]
/	Biatractylolide	PC12 and SH-SY5Y cell (glutamate-induced)	Cell viability; Cell apoptosis; LDA; Protein expression	10, 15, 20 μM	PI3K-Akt-GSK3β-Dependent Pathways	GSK3β protein expression ↓; p-Akt protein expression ↑	[67]
Parkinson's Disease	AT-I	BV-2 cells (LPS-induced); Male C57BL6/J mice (MPTP-intoxicated)	mRNA and protein levels; Immunocytochemistry; Immunohistochemistry;	25, 50, 100 μM (for cells); 3, 10, 30 mg/kg/mL (for rats)	/	NF-κB ↓; HO-1 ↑; MnSOD ↑; TH-immunoreactive neurons ↑; Microglial activation ↓	[68]
Anti depressant like effect	AT-I	Male ICR mice (CUMS induced depressive like behaviors)	Hippocampal neurotransmitter levels; Hippocampal pro inflammatory cytokine levels; NLRP3 inflammasome in the hippocampi	5, 10, 20 mg/kg	/	Serotonin ↓; Norepinephrine ↓; NLRP3 inflammasome ↓; (IL)-1β ↓	[69]
Alzheimer's disease	Biatractylenolide II	/	AChE inhibitory activities; Molecular docking	/	/	Biatractylenolide II can interact with PAS and CAS of AChE	[70]
Cerebral ischemic injury and neuroinflammation	AT-III	Male C57BL/6J mice (MCAO- induced); Primary microglia (OGDR stimulation)	Brain infarct size; Cerebral blood flow; Brain edema; Neurological deficits; Protein expressions of proinflammatory; Anti-inflammatory cytokines	0.01, 0.1, 1, 10, 100 μM (for cells); 0.1–10 mg/kg (for rats)	JAK2/STAT3/Drp 1-dependent mitochondrial fission	Brain infarct size ↓; Restored CBF; ameliorated brain edema; Improved neurological deficits; IL-1β ↓; TNF-α ↓; IL-6 ↓; Drp1 phosphorylation ↓	[71]
Reduces depressive- and anxiogenic-like behaviors	AT-III	Male SD rats (LPS-induced and CUMS rat model)	Forced swimming test; Open field test; Sucrose preference test; Novelty-suppressed feeding test; Proinflammatory cytokines levels	3, 10, 30 mg/kg	/	30 mg/kg AT-III produced an anxiolytic-like effect; Prevented depressive- and anxiety-like behaviors; Proinflammatory cytokines levels ↓	[72]
Alleviates injury in rat hippocampal neurons	AT-III	Male SD rats (isoflurane-induced)	Apoptosis and autophagy in the hippocampal neurons; Inflammatory factors; Levels of p-PI3K, p-Akt, p-mTOR	1.2, 2.4, 4.8 mg/kg	PI3K/Akt/mTOR signaling pathway	TNF-α ↓; IL-1β ↓; IL-6 ↓; p-PI3K ↑; p-Akt ↑; p-mTOR ↑	[73]

"/" denotes no useful information found in the study.

biatractylenolide II was measured, and molecular simulations were also performed. It was found to interact with the peripheral anion site and active catalytic site of AChE[70]. AT-III has a broader neuroprotective function. The middle cerebral artery (MCAO) mouse model and oxygen-glucose deprivation-reoxygenation (OGDR) microglia model were constructed. AT-III was found to ameliorate brain edema and neurological deficits in MCAO mice. In addition, AT-III suppressed neuroinflammation and reduced ischemia-related complications through JAK2/STAT3-dependent mitochondrial fission in microglia[71]. In order to investigate the anti-depressant and anti-anxiolytic effects of AT-III, the LPS-induced depression model and CUMS model were constructed. Combined with the sucrose preference test (SPT), novelty-suppressed feeding test (NSFT), and forced swimming test (FST) to demonstrate that AT-III has anti-depressant and anti-anxiolytic functions by inhibiting hippocampal neuronal inflammation[72]. In addition, AT-III also has the effect of attenuating hippocampal neuronal injury in rats. An isoflurane-induced SD rats injury model was constructed. AT-III alleviated apoptosis, autophagy, and inflammation in hippocampal neurons suggesting that AT-III can play a role in anesthesia-induced neurological injury[73]. However, AT-III attenuates anesthetic-induced neurotoxicity is not known.

Immunomodulatory and anti-inflammatory activity

Immunomodulatory and anti-inflammatory activities are studied *in vivo* and *in vitro*. The construction of an inflammatory cell model *in vitro* generally uses RAW 264.7 macrophages. Different cells, such as BV2 microglia, MG6 cells, and IEC-6 cells, can also be used. Active compounds' immune and anti-inflammatory activity is generally examined using LPS-induced cell and mouse models. For enteritis, injury induction is performed using TNBS and DSS. Several studies have shown that AT-III has immunomodulatory and anti-inflammatory activities. Other sesquiterpene compounds also exhibit certain activities. The related biological activities, animal models, monitoring indicators, and results are summarized in Table 4. For example, five new sesquiterpene compounds, atractylmacrols A-E, were isolated from AMR. The anti-inflammatory effect of the compounds was examined with LPS-induced RAW264.7 macrophage damage, and atractylmacrols A-E were found to inhibit NO production[74]. Three compounds, 2-[(2E)-3,7-dimethyl-2,6-octadienyl]-6-methyl-2, 5-cyclohexadiene-1, 4-dione (1); 1-acetoxy-tetradeca-6E,12E-diene-8, 10-diyne-3-ol (2); 1,3-diacetoxy-tetradeca-6E, 12E-diene-8,10-diyne (3) were isolated from AMR. All three compounds could inhibit the transcriptional activity and nuclear translocation of NF-κB. The most active compound was compound 1, which reduced pro-inflammatory cytokines and inhibited MAPK phosphorylation[75]. Twenty-two compounds were identified from AMR. LPS-induced RAW 264.7 macrophages and BV2 cell injury models were constructed, respectively. Among them, three compounds, AT-I, AT-II, and 8-epiasterolid showed significant damage protection in both cell models and inhibited LPS-induced cell injury by inactivating the NF-κB signaling pathway[76]. To construct a TNBS-induced mouse colitis model, AT-III regulated oxidative stress through FPR1 and Nrf2 signaling pathways, alleviated the upregulation of FPR1 and Nrf2 proteins, and reduced the abundance of *Lactobacilli* in injured mice[77]. AT-III also has anti-inflammatory effects in peripheral organs. A model of LPS-injured MG6 cells was constructed. AT-III alleviated LPS injury by significantly reducing the mRNA expression of TLR4 and inhibiting the p38 MAPK and JNK pathways[78]. It indicated that AT-III has the potential as a therapeutic agent for encephalitis. The neuroprotective and anti-inflammatory effects of AT-III were investigated in a model of LPS-induced BV2 cell injury and a spinal

Table 4. Immunomodulatory and anti-inflammatory activities of esters and sesquiterpenoids.

Activities	Substance	Model	Index	Dose	Signal pathway	Result	Ref.
Against LPS-induced NO production	Atractylmacrols A-E	RAW264.7 macrophages (LPS-induced)	Isolation; Structural identification; Inhibition activity of NO production	25 μM	/	Have effects on LPS-induced NO production	[74]
Anti-inflammatory	2-[(2E)-3,7-dimethyl-2,6-octadienyl]-6-methyl-2,5-cyclohexadiene-1, 4-dione; 1-acetoxy-tetradeca-6E,12E-diene-8, 10-diyne-3-ol; 1,3-diacetoxy-tetradeca-6E, 12E-diene-8, 10-diyne	RAW 264.7 macrophages (LPS-induced)	Level of NO and PGE2; Level of iNOS, COX-2; Levels of pro-inflammatory cytokines; Phosphorylation of MAPK(p38, JNK, and ERK1/2)	2 and 10 μM	NF-κB signaling pathway	IL-1β ↓; IL-6 ↓; TNF-α ↓; p38 ↓; JNK ↓; ERK1/2 ↓	[75]
Anti-inflammatory	AT-I; AT-II; 8-epiasterolid	RAW264.7 macrophages; BV2 microglial cells (LPS-induced)	Structure identification; NO, PGE2 production; Protein expression of iNOS, COX-2, and cytokines	40 and 80 μM	NF-κB signaling pathway.	NO ↓; PGE2 ↓; iNOS ↓; COX-2 ↓; IL-1β ↓; IL-6 ↓; TNF-α ↓	[76]
Intestinal inflammation	AT-III	Male C57BL/6 mice (TNBS-induced)	Levels of myeloperoxidase; Inflammatory factors; Levels of the prooxidant markers, reactive oxygen species, and malondialdehyde; Antioxidant-related enzymes; Intestinal flora	5, 10, 20 mg/kg	FPR1 and Nrf2 pathways	Disease activity index score ↓; Myeloperoxidase ↓; Inflammatory factors interleukin-1β ↓; Tumor necrosis factor-α ↓; Antioxidant enzymes catalase ↓; Superoxide dismutase ↓; Glutathione peroxidase ↓; FPR1 and Nrf2 ↑; Lactobacilli ↓	[77]
Anti-inflammatory	AT-III	MG6 cells (LPS-induced)	mRNA and protein levels of TLR4, TNF-α, IL-1β, IL-6, iNOS, COX-2; Phosphorylation of p38 MAPK and JNK	100 μM	p38 MAPK and JNK signaling pathways	TNF-α ↓; IL-1β ↓; IL-6 ↓; iNOS ↓; COX-2 ↓	[78]
Ameliorates spinal cord injury	AT-III	BV2 microglial (LPS-induced); Female SD rats (Infinite Horizon impactor)	Spinal cord lesion area; Myelin integrity; Surviving neurons; Locomotor function; Microglia/macrophages; Inflammatory factors	1, 10, 100 μM (for cell); 5 mg/kg (for rats)	NF-κB, JNK MAPK, p38 MAPK, and Akt pathways	Active microglia/macrophages; Inflammatory mediators ↓	[79]
Ulcerative colitis	AT-III	IEC-6 (LPS-induced); C57BL/6J male mice (DSS-induced)	MDA,GSH content; SOD activity; Intestinal permeability; Mitochondrial membrane potential; Complex I and complex IV activity	40 and 80 μM (for cell); 5 and 10 mg/kg (for rats)	AMPK/ SIRT1/PGC-1α signaling pathway	Disease activity index ↓; p-AMPK ↑; SIRT1 ↑; PGC-1α ↑; Acetylated PGC-1α ↑	[80]

'/' denotes no useful information found in the study.

cord injury (SCI) mouse model. AT-III alleviated the injury in SCI rats, promoted the conversion of M1 to M2, and attenuated the activation of microglia/macrophages, probably through NF-κB, JNK MAPK, p38 MAPK, and Akt signaling pathways[79]. AT-III has a protective effect against UC. DSS-induced mouse model and LPS-induced IEC-6 cell injury model were constructed. AT-III alleviated DSS and LPS-induced mitochondrial dysfunction by activating the AMPK/SIRT1/PGC-1α signaling pathway[80].

Sesquiterpene biosynthetic pathways in *A. macrocephala*

The biosynthetic pathways for bioactive compounds of *A. macrocephala* are shown in Fig. 6. The biosynthetic pathways of all terpenes include the mevalonate (MVA) pathway in the cytosol and the 2-C-methyl-D-erythritol 4-phosphate (MEP) pathway in the plastid[81]. The cytosolic MVA pathway is started with the primary metabolite acetyl-CoA and supplies isopentenyl (IPP), and dimethylallyl diphosphate (DMAPP) catalyzed by six enzymatic steps, including acetoacetyl-CoA thiolase (AACT), hydroxymethylglutaryl-CoA synthase (HMGS), hydroxymethylglutaryl-CoA reductase (HMGR), mevalonate kinase (MVK), phosphomevalonate kinase (PMK) and mevalonate 5-phosphate decarboxylase (MVD)[82]. IPP and DMAPP can be reversibly isomerized by isopentenyl diphosphate isomerase (IDI)[83]. In the MEP pathway, D-glyceraldehyde-3-phosphate (GAP) and pyruvate are transformed into IPP and DMAPP over seven enzymatic steps, including 1-deoxy-d-xylulose 5-phosphate synthase (DXS), 1-deoxy-d-xylulose 5-phosphate reductoisomerase (DXR), 2C-methyl-d-erythritol 4-phosphate cytidyltransferase(MECT),4-(cytidine5′-diphospho)-2C-methyl-d-erythritol kinase (CMK), 2C-methyl-d-erythritol-2,4-cyclodiphosphate synthase (MECP), 4-hydroxy-3-methylbut-2-enyl diphosphate synthase (HDS) and 4-hydroxy-3-methylbut-2-enyl diphosphate reductase (HDR) were involved in the whole process[84]. The common precursor of sesquiterpenes is farnesyl diphosphate (FPP) synthesized from IPP and DMAPP under the catalysis of farnesyl diphosphate synthase (FPPS)[85]. Various sesquiterpene synthases, such as β-farnesene synthase (β-FS), germacrene A synthase (GAS), β-caryophyllene synthase (QHS), convert the universal precursor FPP into more than 300 different sesquiterpene skeletons in different species[86–89]. Unfortunately, in *A. macrocephala*, only the functions of AmF-PPS in the sesquiterpenoid biosynthetic pathway have been validated *in vitro*[90]. Identifying sesquiterpene biosynthesis in *A. macrocephala* is difficult due to the lack of: isotope-labeled biosynthetic pathways, constructed genetic transformation system, and high-quality genome.

Technology application in *A. macrocephala*

Transcriptome sequencing in *A. macrocephala*

With the gradual application of transcriptome sequencing technology in the study of some non-model plants, the study of *A. macrocephala* has entered the stage of advanced genetics and genomics. Yang et al. determined the sesquiterpene content in the volatile oil of AMR by gas chromatography and mass spectrometry (GC-MS) in *A. macrocephala*. Mixed samples of leaves, stems, rhizomes, and flowers of *A. macrocephala* were sequenced by Illumina high throughput sequencing technology[91]. Similarly, compounds' relative content in five *A. macrocephala* tissue was quantitatively detected by ultra-performance liquid chromatography-tandem mass spectrometry. Sesquiterpenoids accumulations in rhizomes and roots were reported[90]. Seventy-three terpenoid skeleton synthetases and 14 transcription factors highly expressed in rhizomes were identified by transcriptome analysis. At the same time, the function of AmFPPS related to the terpenoid synthesis pathway in *A. macrocephala* was verified *in vitro*[90]. In addition to the study of the different tissue parts of *A. macrocephala*, the different origin of *A. macrocephala* is also worthy of attention. The AMR from different producing areas was sequenced by transcriptome. Seasonal effects in *A. macrocephala* were also studied. Interestingly, compared with one-year growth AMR, the decrease of terpenes and polyketone metabolites in three-year growth AMR was correlated with the decreased expression of terpene synthesis genes[92]. Infestation of *Sclerotium rolfsii sacc (S. rolfsii)* is one of the main threats encountered in producing *A. macrocephala*[93]. To explore the expression changes of *A. macrocephala*-related genes after chrysanthemum indicum polysaccharide (CIP) induction, especially those related to defense, the samples before and after treatment were

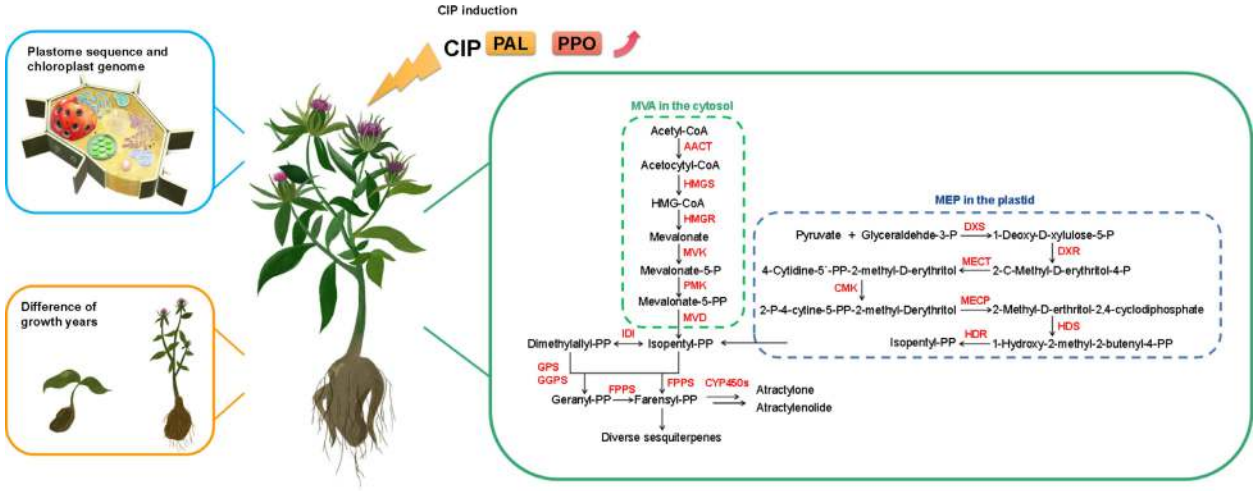

Fig. 6 Biosynthetic pathways for bioactive compounds of *A. macrocephala*.

sequenced. The expression levels of defense-related genes, such as polyphenol oxidase (PPO) and phenylalanine ammonia-lyase (PAL) genes, were upregulated in *A. macrocephala* after CIP treatment[94].

Metabolomics analysis in *A. macrocephala*

Traditional Chinese Medicine (TCM), specifically herbal medicine, possesses intricate chemical compositions due to both primary and secondary metabolites that exhibit a broad spectrum of properties, such as acidity-base, polarity, molecular mass, and content. The diverse nature of these components poses significant challenges when conducting quality investigations of TCM[95]. Recent advancements in analytical technologies have contributed significantly to the profiling and characterizing of various natural compounds present in TCM and its compound formulae. Novel separation and identification techniques have gained prominence in this regard. The aerial part of *A. macrocephala* (APA) has been studied for its anti-inflammatory and antioxidant properties. The active constituents have been analyzed using high-performance liquid chromatography-electrospray ionization-tandem mass spectrometry (HPLC-ESI-MS/MS). The results indicated that APA extracts and all sub-fractions contain a rich source of phenolics and flavonoids. The APA extracts and sub-fractions (particularly ACE 10-containing constituents) exhibited significant anti-inflammatory and antioxidant activity[96]. In another study, a four-dimensional separation approach was employed using offline two-dimensional liquid chromatography ion mobility time-of-flight mass spectrometry (2D-LC/IM-TOF-MS) in combination with database-driven computational peak annotation. A total of 251 components were identified or tentatively characterized from *A. macrocephala*, including 115 sesquiterpenoids, 90 polyacetylenes, 11 flavonoids, nine benzoquinones, 12 coumarins, and 14 other compounds. This methodology significantly improved in identifying minor plant components compared to conventional LC/MS approaches[97]. Activity-guided separation was employed to identify antioxidant response element (ARE)-inducing constituents from the rhizomes of dried *A. macrocephala*. The combination of centrifugal partition chromatography (CPC) and an ARE luciferase reporter assay performed the separation. The study's results indicate that CPC is a potent tool for bioactivity-guided purification from natural products[98]. In addition, ^{1}H NMR-based metabolic profiling and genetic assessment help identify members of the Atractylodes genus[99]. Moreover, there were many volatile chemical compositions in *A. macrocephala*. The fatty acyl composition of seeds from *A. macrocephala* was determined by GC-MS of fatty acid methyl esters and 3-pyridylcarbinol esters[100]. Fifteen compounds were identified in the essential oil extracted from the wild rhizome of Qimen *A. macrocephala*. The major components identified through gas chromatography-mass spectrometry (GC-MS) analysis were atractylone (39.22%) and β-eudesmol (27.70%). Moreover, gas purge microsolvent extraction (GP-MSE) combined with GC-MS can effectively characterize three species belonging to the Atractylodes family (*A. macrocephala*, *A. japonica*, and *A. lancea*)[101].

Conclusions and perspectives

So far, the research on *A. macrocephala* has focused on pharmacological aspects, with less scientific attention to biogeography, PAO-ZHI processing, biosynthesis pathways for bioactive compounds, and technology application. The different origins lead to specific differences in appearance, volatile oil content, volatile oil composition, and relative percentage content of *A. macrocephala*. However, *A. macrocephala* resources lack a systematic monitoring system regarding origin traceability and quality control, and there is no standardized process for origin differentiation. Besides, the PAO-ZHI processing of *A. macrocephala* is designed to reduce toxicity and increase effectiveness. The active components will have different changes before and after processing. But current research has not been able to decipher the mechanism by which the processing produces its effects. Adaptation of *in vivo* and *in vitro* can facilitate understanding the biological activity. The choice of the models and doses is particularly important. The recent studies that identified AMR bioactivities provided new evidence but are somewhat scattered. For example, in different studies, the same biological activity corresponds to different signaling pathways, but the relationship between the signaling pathways has not been determined. Therefore, a more systematic study of the various activities of AMR is one of the directions for future pharmacological activity research of *A. macrocephala*. In addition, whether there are synergistic effects among the active components in AMR also deserves further study, but they are also more exhaustive. As for the biosynthesis of bioactive compounds in *A. macrocephala*, the lack of isotopic markers, mature genetic transformation systems, and high-quality genomic prediction of biosynthetic pathways challenge the progress in sesquiterpene characterization. In recent years, the transcriptomes of different types of *A. macrocephala* have provided a theoretical basis and research foundation for further exploration of functional genes and molecular regulatory mechanisms but still lack systematicity. Ulteriorly, applying new technologies will gradually unlock the mystery of *A. macrocephala*.

Acknowledgments

This work was supported by the Key Scientific and Technological Grant of Zhejiang for Breeding New Agricultural Varieties (2021C02074), National Young Qihuang Scholars Training Program, National 'Ten-thousand Talents Program' for Leading Talents of Science and Technology Innovation in China, National Natural Science Foundation of China (81522049), Zhejiang Provincial Program for the Cultivation of High level Innovative Health Talents, Zhejiang Provincial Ten Thousands Program for Leading Talents of Science and Technology Innovation (2018R52050), Research Projects of Zhejiang Chinese Medical University (2021JKZDZC06, 2022JKZKTS18). We appreciate the great help/technical support/experimental support from the Public Platform of Pharmaceutical/Medical Research Center, Academy of Chinese Medical Science, Zhejiang Chinese Medical University.

Conflict of interest

The authors declare that they have no conflict of interest.

Dates

Received 16 January 2023; Accepted 18 April 2023; Published online 30 May 2023

References

1. Zou X. 2010. *A pharmacophylogenetic study of Atractylodes plants*. PhD. Dissertation. Beijing University of Chinese Medicine, Beijing.
2. Cai H, Xu Z, Luo S, Zhang W, Cao G, et al. 2012. Study on chemical fingerprinting of crude and processed *Atractylodes macrocephala* from different locations in Zhejiang province by reversed-phase high-performance liquid chromatography coupled with hierarchical cluster analysis. *Pharmacognosy Magazine* 8:300–7
3. Zhu B, Zhang Q, Hua J, Cheng W, Qin L. 2018. The traditional uses, phytochemistry, and pharmacology of *Atractylodes macrocephala* Koidz. : A review. *Journal of Ethnopharmacology* 226:143–67
4. Kohjyouma M, Nakajima S, Namera A, Shimizu R, Mizukami H, et al. 1997. Random amplified polymorphic DNA analysis and variation of essential oil components of Atractylodes plants. *Biological and Pharmaceutical Bulletin* 20:502–6
5. Wu ZY, Raven PH, Hong DY. 2011. *Flora of China*. Beijing: Science Press and St. Louis: Missouri Botanical Garden Press. www.iplant.cn/foc/Guidelines
6. Ma Y, Gao XQ, Song YP. 2000. Technology of harvest, process, and preparation of *Atractylodes macrocephala* Koidz. *Lishizhen Medicine and Materia Medica Research* 11:307
7. Editorial Committee of Chinese Pharmacopoeia. 2020. *Pharmacopoeia of the People's Republic of China*. pp 107. Beijing: China Medical Science and Technology Press
8. Yang Y, Wei N, Wu Y, Yang S, Xie J, et al. 2021. Research progress on extraction separation, chemical constitution and pharmacological activities of polysaccharide extracted from *Atractylodes macrocephala*. *Chinese Traditional and Herbal Drugs* 50:578–84
9. Houpan S. 2014. *Studies on the effects of Atractylodes macrocephala Koidz. on polyamine-mediated calcium channels signaling pathway during intestinal epithelial cell migration*. PhD. Dissertation. Guangzhou University of Chinese Medicine, Guangzhou
10. Deng M, Chen H, Long J, Song J, Xie L, et al. 2021. Atractylenolides (I, II, and III): a review of their pharmacology and pharmacokinetics. *Archives of Pharmacal Research* 44:633–54
11. Bailly C. 2021. Atractylenolides, essential components of Atractylodes-based traditional herbal medicines: Antioxidant, anti-inflammatory and anticancer properties. *European Journal of Pharmacology* 891:173735
12. Zheng L, Shao ZD, Wang ZC, Fu CX. 2012. Isolation and characterization of polymorphic microsatellite markers from the Chinese medicinal herb *Atractylodes macrocephala* (Asteraceae). *International Journal of Molecular Sciences* 13:16046–52
13. Peng W, Han T, Xin WB, Zhang XG, Zhang QY, et al. 2011. Comparative research of chemical constituents and bioactivities between petroleum ether extracts of the aerial part and the rhizome of *Atractylodes macrocephala*. *Medicinal Chemistry Research* 20:146–51
14. Peng H, Wang D. 2004. Formation and changes of atractylodes root medicine. *Chinese Journal of Traditional Chinese Medicine* 12:1133-113–15-17
15. Yang S, Gong H, Zhao Y, Chen B, Fu C. 2013. Effects of origin and provenance on the quality of Atractylodes Rhizoma. *Journal of Chinese Medicinal Materials* 36(6):890–92
16. Zhu X, Song R, Wu Z, Zhou J, Cao L, et al. 2015. Standard cultivation of atractylodes in Pingjiang County, Hunan Province. *Chinese Journal of Tropical Agriculture* 35:19–22
17. Chen W, Wang H, Wang T, Chang Y, Chen Y, et al. 2022. Three-dimensional fluorescence combined with chemometrics for origin tracing of Atractylodes Rhizoma. *Spectroscopy and Spectral Analysis* 42:2875–83
18. Zhang L, Qin J, Zhao W, Ma H, Chen X, et al. 2019. A Study on the Identification of Atractylodes Rhizoma from Different Origins. *Anhui Agricultural Sciences* 47(203-6):203–206,254
19. Guo L, Mo R, Tan Y, Pan Y, Chen D. 2021. Analysis of differentially expressed genes in the transcriptome of Atractylodes macrocephala from different origins. *Journal of Chinese Medicinal Materials* 44(12):2787–92
20. Zhou J, Deng Z, Chen M, Xiao S, Zhou H, et al. 2022. Changes of chlorogenic acid content in neochlorogenic acid before and after processing of Atractylodes Rhizoma from different origins. *Chinese Modern Chinese Medicine* 24(12):2471–75
21. Gu S, Li L, Huang H, Wang B, Zhang T. 2019. Antitumor, antiviral, and anti-Inflammatory efficacy of essential oils from *Atractylodes macrocephala* Koidz. produced with different processing methods. *Molecules* 24(16):2956
22. Xu S, Qi X, Liu Y, Liu Y, Lv X, et al. 2018. UPLC-MS/MS of Atractylenolide I, Atractylenolide II, Atractylenolide III, and Atractyloside A in rat plasma after oral administration of raw and wheat bran-processed atractylodis rhizoma. *Molecules* 23(12):3234
23. Sun X, Cui X, Wen H, Shan C, Wang X, et al. 2017. Influence of sulfur fumigation on the chemical profiles of *Atractylodes macrocephala* Koidz. evaluated by UFLC-QTOF-MS combined with multivariate statistical analysis. *Journal of Pharmaceutical and Biomedical Analysis* 141:19–31
24. Hwang MH, Seo JW, Han KJ, Kim MJ, Seong ES. 2022. Effect of artificial light treatment on the physiological property and biological activity of the aerial and underground parts of *Atractylodes macrocephala*. *Agronomy* 12:1485
25. Hwang MH, Seo JW, Park BJ, Han KJ, Lee JG, et al. 2022. Evaluation of growth characteristics and biological activities of 'Dachul', a hybrid medicinal plant of *Atractylodes macrocephala* × *Atractylodes japonica*, under different artificial light sources. *Plants* 11(15):2035
26. Zhou Y, Lu X, Chen L, Zhang P, Zhou J, et al. 2021. Polysaccharides from *Chrysanthemun indicum* L. enhance the accumulation of polysaccharide and atractylenolide in *Atractylodes macrocephala* Koidz. *International Journal of Biological Macromolecules* 190:649–59
27. Du N, Tian W, Zheng D, Zhang X, Qin P. 2016. Extraction, purification and elicitor activities of polysaccharides from *Chrysanthemum indicum*. *International Journal of Biological Macromolecules* 82:347–54
28. Xue W, Gao Y, Li Q, Lu Q, Bian Z, et al. 2020. Immunomodulatory activity-guided isolation and characterization of a novel polysaccharide from *Atractylodis macrocephalae* Koidz. *International Journal of Biological Macromolecules* 161:514–24
29. Cui YS, Li YX, Jiang SL, Song AN, Fu Z, et al. 2020. Isolation, purification, and structural characterization of polysaccharides from *Atractylodis Macrocephalae* rhizoma and their immunostimulatory activity in RAW264.7 cells. *International Journal of Biological Macromolecules* 163:270–8
30. Xu W, Guan R, Shi F, Du A, Hu S. 2017. Structural analysis and immunomodulatory effect of polysaccharide from *Atractylodis macrocephalae* Koidz. on bovine lymphocytes. *Carbohydrate Polymers* 174:1213–23
31. Feng Y, Ji H, Dong X, Yu J, Liu A. 2019. Polysaccharide extracted from *Atractylodes macrocephala* Koidz (PAMK) induce apoptosis in transplanted H22 cells in mice. *International Journal of Biological Macromolecules* 137:604–11
32. Miao YF, Gao XN, Xu DN, Li MC, Gao ZS, et al. 2021. Protective effect of the new prepared *Atractylodes macrocephala* Koidz polysaccharide on fatty liver hemorrhagic syndrome in laying hens. *Poultry Science* 100:938–48
33. Guo S, Li W, Chen F, Yang S, Huang Y, et al. 2021. Polysaccharide of *Atractylodes macrocephala* Koidz regulates LPS-mediated mouse hepatitis through the TLR4-MyD88-NFκB signaling pathway. *International Immunopharmacology* 98:107692
34. Wang R, Shan H, Zhang G, Li Q, Wang J, et al. 2022. An inulin-type fructan (AMP1-1) from *Atractylodes macrocephala* with anti-weightlessness bone loss activity. *Carbohydrate Polymers* 294:119742

35. Xu D, Li B, Cao N, Li W, Tian Y, et al. 2017. The protective effects of polysaccharide of *Atractylodes macrocephala* Koidz. (PAMK) on the chicken spleen under heat stress via antagonizing apoptosis and restoring the immune function. *Oncotarget* 8:70394–405
36. Xu D, Li W, Li B, Tian Y, Huang Y. 2017. The effect of selenium and polysaccharide of *Atractylodes macrocephala* Koidz. (PAMK) on endoplasmic reticulum stress and apoptosis in chicken spleen induced by heat stress. *RSC Advances* 7:7519–25
37. Li W, Guo S, Xu D, Li B, Cao N, et al. 2018. Polysaccharide of *Atractylodes macrocephala* Koidz (PAMK) relieves immunosuppression in cyclophosphamide-treated geese by maintaining a humoral and cellular immune balance. *Molecules* 23(4):932
38. Li W, Xiang X, Cao N, Chen W, Tian Y, et al. 2021. Polysaccharide of *Atractylodes macrocephala* koidz activated T lymphocytes to alleviate cyclophosphamide-induced immunosuppression of geese through novel_mir2/CD28/AP-1 signal pathway. *Poultry Science* 100:101129
39. Li W, Xu D, Li B, Cao N, Guo S, et al. 2018. The polysaccharide of *Atractylodes macrocephala* koidz (PAMK) alleviates cyclophosphamide-mediated immunosuppression in geese, possibly through novel_mir2 targeting of CTLA4 to upregulate the TCR-NFAT pathway. *RSC Advances* 8:26837–48
40. Xiang X, Cao N, Chen F, Qian L, Wang Y, et al. 2020. Polysaccharide of *Atractylodes macrocephala* Koidz (PAMK) alleviates cyclophosphamide-induced immunosuppression in mice by upregulating CD28/IP3R/PLCγ-1/AP-1/NFAT signal pathway. *Frontiers in Pharmacology* 11:529657
41. Li BX, Li WY, Tian YB, Guo SX, Huang YM, et al. 2019. Polysaccharide of *Atractylodes macrocephala* Koidz enhances cytokine secretion by stimulating the *TLR4-MyD88-NF-κB* signaling pathway in the mouse spleen. *Journal of Medicinal Food* 22:937–43
42. Xu W, Fang S, Cui X, Guan R, Wang Y, et al. 2019. Signaling pathway underlying splenocytes activation by polysaccharides from *Atractylodis macrocephalae* Koidz. *Molecular Immunology* 111:19–26
43. Xu W, Fang S, Wang Y, Zhang T, Hu S. 2020. Molecular mechanisms associated with macrophage activation by *Rhizoma Atractylodis Macrocephalae* polysaccharides. *International Journal of Biological Macromolecules* 147:616–28
44. Wu Q, Li B, Li Y, Liu F, Yang L, et al. 2022. Effects of PAMK on lncRNA, miRNA, and mRNA expression profiles of thymic epithelial cells. *Functional & Integrative Genomics* 22:849–63
45. Xu W, Fang S, Wang Y, Chi X, Ma X, et al. 2020. Receptor and signaling pathway involved in bovine lymphocyte activation by *Atractylodis macrocephalae* polysaccharides. *Carbohydrate Polymers* 234:115906
46. Liu Z, Sun Y, Zhang J, Ou N, Gu P, et al. 2018. Immunopotentiation of polysaccharides of *Atractylodes macrocephala* Koidz-loaded nanostructured lipid carriers as an adjuvant. *International Journal of Biological Macromolecules* 120:768–74
47. Sun Y, Zhang J, Bo R, Ou N, Gu P, et al. 2018. Polysaccharides of *Atractylodes macrocephala* Koidz-loaded nanostructured lipid carriers: optimization on conditions by RSM and immunological activity in vitro. *Journal of Drug Delivery Science and Technology* 44:305–13
48. Li W, Xiang X, Li B, Wang Y, Qian L, et al. 2021. PAMK relieves LPS-Induced enteritis and improves intestinal flora disorder in goslings. *Evidence-Based Complementary and Alternative Medicine* 2021:9721353
49. Feng W, Liu J, Tan Y, Ao H, Wang J, et al. 2020. Polysaccharides from *Atractylodes macrocephala* Koidz. ameliorate ulcerative colitis via extensive modification of gut microbiota and host metabolism. *Food Research International* 138:109777
50. Kai L, Zong X, Jiang Q, Lu Z, Wang F, et al. 2022. Protective effects of polysaccharides from *Atractylodes macrocephalae* Koidz. against dextran sulfate sodium induced intestinal mucosal injury on mice. *International Journal of Biological Macromolecules* 195:142–51
51. Zong X, Xiao X, Kai L, Cheng Y, Fu J, et al. 2021. *Atractylodis macrocephalae* polysaccharides protect against DSS-induced intestinal injury through a novel lncRNA ITSN1-OT1. *International Journal of Biological Macromolecules* 167:76–84
52. Zheng Z, Wang J. 2022. Bone marrow mesenchymal stem cells combined with *Atractylodes macrocephala* polysaccharide attenuate ulcerative colitis. *Bioengineered* 13:824–33
53. Feng Y, Ji H, Dong X, Liu A. 2019. An alcohol-soluble polysaccharide from *Atractylodes macrocephala* Koidz induces apoptosis of Eca-109 cells. *Carbohydrate Polymers* 226:115136
54. Feng Z, Yang R, Wu L, Tang S, Wei B, et al. 2019. *Atractylodes macrocephala* polysaccharides regulate the innate immunity of colorectal cancer cells by modulating the TLR4 signaling pathway. *OncoTargets and Therapy* 12:7111–21
55. Zhang D, Li X, Song D, Chen S, Zhang Z, et al. 2022. Atractylenolide III induces apoptosis by regulating the Bax/Bcl-2 signaling pathway in human colorectal cancer HCT-116 Cells *in vitro* and *in vivo*. *Anti-cancer Drugs* 33:30–47
56. Tian S, Yu H. 2017. Atractylenolide II Inhibits proliferation, motility and induces apoptosis in human gastric carcinoma cell lines HGC-27 and AGS. *Molecules* 22(11):1886
57. Wang T, Long F, Zhang X, Yang Y, Jiang X, Wang L. 2017. Chemopreventive effects of atractylenolide II on mammary tumorigenesis via activating Nrf2-ARE pathway. *Oncotarget* 8:77500–14
58. Chan KWK, Chung HY, Ho WS. 2020. Anti-tumor activity of Atractylenolide I in human colon adenocarcinoma *in vitro*. *Molecules* 25(1):212
59. Wang M, Li XZ, Zhang MX, Ye QY, Chen YX, Chang X. 2021. Atractylenolide-I sensitizes triple-negative breast cancer cells to paclitaxel by blocking CTGF expression and fibroblast activation. *Frontiers in Oncology* 11:738534
60. Long F, Wang T, Jia P, Wang H, Qing Y, et al. 2017. Anti-tumor effects of Atractylenolide-I on human ovarian cancer cells. *Medical Science Monitor* 23:571–79
61. Tang D, Xu X, Ying J, Xie T, Cao G. 2020. Transfer of metastatic traits via miR-200c in extracellular vesicles derived from colorectal cancer stem cells is inhibited by atractylenolide I. *Clinical and Translational Medicine* 10:e139
62. Li Y, Wang Y, Liu Z, Guo X, Miao Z, et al. 2020. Atractylenolide I induces apoptosis and suppresses glycolysis by blocking the JAK2/STAT3 signaling pathway in colorectal cancer cells. *Frontiers in Pharmacology* 11:273
63. Xiao Q, Zheng F, Wu J, Tang Q, Wang W, et al. 2017. Activation of ERK and mutual regulation of Stat3 and SP1 contribute to inhibition of PDK1 expression by Atractylenolide-1 in human lung cancer cells. *Cellular Physiology and Biochemistry* 43:2353–66
64. Zhang N, Liu C, Sun TM, Ran XK, Kang TG, et al. 2017. Two new compounds from *Atractylodes macrocephala* with neuroprotective activity. *Journal of Asian Natural Products Research* 19:35–41
65. Si JG, Zhang HX, Yu M, Li LY, Zhang HW, et al. 2021. Sesquiterpenoids from the rhizomes of *Atractylodes macrocephala* and their protection against lipopolysaccharide-induced neuroinflammation in microglia BV-2 cells. *Journal of Functional Foods* 83:104541
66. Zhao TY, Liu ZQ, Ma SF, Bo Y, Guo FF, et al. 2020. Biatractylolide reduced amyloid beta protein-induced memory impairment in rats. *Pakistan Journal of Zoology* 52:1031–38
67. Zhu L, Ning N, Li Y, Zhang QF, Xie YC, et al. 2017. Biatractylolide modulates PI3K-Akt-GSK3β-dependent pathways to protect against glutamate-induced cell damage in PC12 and SH-SY5Y cells. *Evidence-Based Complementary and Alternative Medicine* 2017:1291458

68. More S, Choi DK. 2017. Neuroprotective role of Atractylenolide-I in an *in vitro* and *in vivo* model of Parkinson's disease. *Nutrients* 9(5):451
69. Gao H, Zhu X, Xi Y, Li Q, Shen Z, et al. 2018. Anti-depressant-like effect of atractylenolide I in a mouse model of depression induced by chronic unpredictable mild stress. *Experimental and Therapeutic Medicine* 15:1574–79
70. Zhu Q, Lin M, Zhuo W, Li Y. 2021. Chemical Constituents from the wild *Atractylodes macrocephala* Koidz and acetylcholinesterase inhibitory activity evaluation as well as molecular docking study. *Molecules* 26(23):7299
71. Zhou K, Chen J, Wu J, Wu Q, Jia C, et al. 2019. Atractylenolide III ameliorates cerebral ischemic injury and neuroinflammation associated with inhibiting JAK2/STAT3/Drp1-dependent mitochondrial fission in microglia. *Phytomedicine* 59:152922
72. Zhou Y, Huang S, Wu F, Zheng Q, Zhang F, et al. 2021. Atractylenolide III reduces depressive-and anxiogenic-like behaviors in rat depression models. *Neuroscience Letters* 759:136050
73. Zhu S, Wang Z, Yu J, Yin L, Zhu A. 2021. Atractylenolide III alleviates isoflurane-induced injury in rat hippocampal neurons by activating the PI3K/Akt/mTOR pathway. *Journal of Food Biochemistry* 45:e13892
74. Wang SY, Ding LF, Su J, Peng LY, Song LD, Wu XD. 2018. Atractylmacrols A-E, sesquiterpenes from the rhizomes of *Atractylodes macrocephala*. *Phytochemistry Letters* 23:127–31
75. Jeong D, Dong GZ, Lee HJ, Ryu JH. 2019. Anti-Inflammatory compounds from *Atractylodes macrocephala*. *Molecules* 24:1859
76. Jin HG, Kim KW, Li J, Lee DY, Yoon D, et al. 2022. Anti-inflammatory components isolated from *Atractylodes macrocephala* in LPS-induced RAW264.7 macrophages and BV2 microglial cells. *Applied Biological Chemistry* 65(1):11
77. Ren Y, Jiang WW, Luo CL, Zhang XH, Huang MJ. 2021. Atractylenolide III ameliorates TNBS-induced intestinal inflammation in mice by reducing oxidative stress and regulating intestinal flora. *Chemistry & Biodiversity* 18(8):e2001001
78. Novianti E, Katsuura G, Kawamura N, Asakawa A, Inui A. 2021. Atractylenolide-III suppresses lipopolysaccharide-induced inflammation via downregulation of toll-like receptor 4 in mouse microglia. *Heliyon* 7:E08269
79. Xue MT, Sheng WJ, Song X, Shi YJ, Geng ZJ, et al. 2022. Atractylenolide III ameliorates spinal cord injury in rats by modulating microglial/macrophage polarization. *CNS Neuroscience & Therapeutics* 28:1059–71
80. Han J, Li W, Shi G, Huang Y, Sun X, et al. 2022. Atractylenolide III Improves mitochondrial function and protects against ulcerative colitis by activating AMPK/SIRT1/PGC-1α. *Mediators of Inflammation* 2022:9129984
81. Frank A, Groll M. 2017. The methylerythritol phosphate pathway to isoprenoids. *Chemical Reviews* 117:5675–703
82. Liao P, Wang H, Hemmerlin A, Nagegowda DA, Bach TJ, et al. 2014. Past achievements, current status and future perspectives of studies on 3-hydroxy-3-methylglutaryl-CoA synthase (HMGS) in the mevalonate (MVA) pathway. *Plant Cell Reports* 33:1005–22
83. Campbell M, Hahn FM, Poulter CD, Leustek T. 1998. Analysis of the isopentenyl diphosphate isomerase gene family from Arabidopsis thaliana. *Plant Molecular Biology* 36:323–28
84. Wright LP, Rohwer JM, Ghirardo A, Hammerbacher A, Ortiz-Alcaide M, et al. 2014. Deoxyxylulose 5-phosphate synthase controls flux through the methylerythritol 4-phosphate pathway in arabidopsis. *Plant Physiology* 165:1488–504
85. Dubey VS, Bhalla R, Luthra R. 2003. An overview of the non-mevalonate pathway for terpenoid biosynthesis in plants. *Journal of Biosciences* 28:637–46
86. Chen F, Wei YX, Zhang JM, Sang XM, Dai CC. 2017. Transcriptomics analysis investigates sesquiterpenoids accumulation pattern in different tissues of Atractylodes lancea (Thunb.) DC. plantlet. *Plant Cell, Tissue and Organ Culture (PCTOC)* 130:73–90
87. Zhao J, Sun C, Shi F, Ma S, Zheng J, et al. 2021. Comparative transcriptome analysis reveals sesquiterpenoid biosynthesis among 1-, 2- and 3-year old Atractylodes chinensis. *BMC Plant Biology* 21:354
88. Ahmed S, Zhan C, Yang Y, Wang X, Yang T, et al. 2016. The Transcript profile of a traditional Chinese medicine, *Atractylodes lancea*, revealing its sesquiterpenoid biosynthesis of the major active components. *PLoS One* 11:e0151975
89. Huang Q, Huang X, Deng J, Liu H, Liu Y, et al. 2016. Differential gene expression between leaf and rhizome in *Atractylodes lancea*: A comparative transcriptome analysis. *Frontiers in Plant Science* 7:348
90. Ruan Q, Wang J, Xiao C, Yang Y, Luo E, et al. 2021. Differential transcriptome analysis of genes associated with the rhizome growth and sesquiterpene biosynthesis in *Atractylodes macrocephala*. *Industrial Crops and Products* 173:114141
91. Yang G, Li H, Jin Y, Dong L, Mo Y, Luo J. 2019. Analysis of genes related to biosynthesis of sesquiterpene in *Atractylodes macrocephala* by transcriptome. *Plant Physiology Journal* 55:1827–38
92. Zhang J, Gu X, Zhao Y, Zheng Y, Wang Q, et al. 2022. Differences in gene expression and endophytic bacterial diversity in *Atractylodes macrocephala* Koidz. rhizomes from different growth years. *Canadian Journal of Microbiology* 68:353–66
93. Jiang J, Feng L, Liu Y, Jiang WD, Hu K, et al. 2013. Mechanistic target of rapamycin in common carp: cDNA cloning, characterization, and tissue expression. *Gene* 512:566–72
94. Zhang P, Zheng F, Chen L, Lu X, Tian W. 2020. CIP elicitors on the defense response of *A. macrocephala* and its related gene expression analysis. *Journal of Plant Physiology* 245:153107
95. Yang W, Zhang Y, Wu W, Huang L, Guo D, et al. 2017. Approaches to establish Q-markers for the quality standards of traditional Chinese medicines. *Acta Pharmaceutica Sinica B* 7:439–46
96. Liu Y, Hu M, Chen L, Su Q. 2019. The anti-inflammatory and antioxidant properties of the aerial part of *Atractylodes macrocephala* and the active constituents' analysis by HPLC-ESI-MS/MS. *South African Journal of Botany* 125:86–91
97. Qian YX, Li WW, Wang HM, Hu WD, Wang HD, et al. 2021. A four-dimensional separation approach by offline 2D-LC/IM-TOF-MS in combination with database-driven computational peak annotation facilitating the in-depth characterization of the multicomponents from *Atractylodis Macrocephalae* rhizoma (*Atractylodes macrocephala*). *Arabian Journal of Chemistry* 14(2):102957
98. Kim MI, Kim JH, Syed AS, Kim YM, Choe KK, et al. 2018. Application of centrifugal partition chromatography for bioactivity-guided purification of antioxidant-response-element-inducing constituents from Atractylodis Rhizoma Alba. *Molecules* 23(9):2274
99. Shirahata T, Ishikawa H, Kudo T, Takada Y, Hoshino A, et al. 2022. Metabolic fingerprinting for discrimination of DNA-authenticated *Atractylodes* plants using ^{1}H NMR spectroscopy. *Journal of Natural Medicines* 75(3):475–88
100. Sun JY, Guo X, Smith MA. 2017. Identification of crepenynic acid in the seed oil of *Atractylodes lancea* and *A. macrocephala*. *Journal of the American Oil Chemists Society* 94:655–60
101. Zhao J, Jin X, Yang C, Quinto M, Shang H, et al. 2020. Gas purge micro solvent extraction: A rapid and powerful tool for essential oil chromatographic fingerprints. *Journal of Pharmaceutical and Biomedical Analysis* 187:113339